Electronic Supplementary Material (ESI) for Chemical Communications.
This journal is © The Royal Society of Chemistry 2022

Supplementary Information

Two Novel Telluroniobates with an Efficient Catalytic Activity for the Imidation/Amidation Reaction

Mengyuan Cheng,[a,+] Yufeng Liu,[b,+] Nan Li,[a,+] Jingwen Shi,[a] Weixin Du,[a] Dongdi Zhang,[a] GuopingYang,*[b] Guan Wang,[a] and Jingyang Niu*[a]*

[a]Henan Key Laboratory of Polyoxometalate Chemistry, College of Chemistry and Chemical Engineering, Henan University, Kaifeng 475004, P. R. China.

[b]Jiangxi Key Laboratory for Mass Spectrometry and Instrumentation, Jiangxi Province Key Laboratory of Synthetic Chemistry, East China University of Technology, Nanchang, 330013, P. R. China.

Content

Experimental section

General methods and materials. $K_7[HNb_6O_{19}]\cdot 13H_2O$ were prepared according to the literature procedure.[S1] Purity was confirmed by IR spectroscopy. All reagents and solvents were of commercially available grade and used without any previous purification. IR spectra were recorded on a Bruker VERTEX 70 IR spectrometer in the 4000-400 cm^{-1} range using crystalline sample in KBr pellet. Elemental analyses were obtained with a PerkinElmer Optima 2100 DV Inductively Coupled Plasma Optical Emission Spectrometry, C, H and N were carried out on a VarioElcube CHNS analyzer. The phase purity of bulk samples was further verified by powder X-ray diffraction (PXRD) patterns collected on a Bruker AXS D8 Advance instrument with Cu Kα radiation (λ = 1.5418 Å). Thermogravimetric analyses (TGA) were carried out on a NETZSCH STA 449 F5 Jupiter thermal analyzer under N_2 atmosphere with 10 °C·min^{-1} heating rate. Negative-mode electrospray ionization mass spectrometry (ESI-MS) of compounds in water were performed on an AB SCIEX Triple TOF 4600 instrument.

CCDC 2097318 and 2097319 contain the supplementary crystallographic data for this paper. These data can be obtained free of charge via www.ccdc.cam.ac.uk/data_request/cif, or by emailing data_request@ccdc.cam.ac.uk, or by contacting The Cambridge Crystallographic Data Centre, 12 Union Road, Cambridge CB2 1EZ, UK; fax: +44 1223 336033.

Catalysis. The products were isolated by column chromatography on silica gel (200-300 mesh) using petroleum ether (60-90 °C) and ethyl acetate. All compounds were characterized by ^{1}H NMR, ^{13}C NMR and mass spectrometry, which were consistent with those reported in related literatures. NMR spectra were determined on Brucker ADVANCE III spectrometer at 500 MHz and 126 MHz. ^{1}H NMR peaks were labeled as singlet (s), doublet (d), triplet (t), and multiplet (m). The coupling constants, J, are reported in Hertz (Hz). GC analysis was performed on Agilent 7890B equipped with a capillary column (HP-5, 30 m × 0.25 μm) using a flame ionization detector. The HR-MS was recorded on an Agilent Q-TOF 6520 equipment.

Synthesis of $Te_{15}Nb_{21}$ and $Te_{10}Nb_{14}$. $[\{Cu(en)_2(H_2O)\}_6][\{Cu(en)_2\}_3][H_3Te_{15}Nb_{21}Cu_3O_{96}]\cdot 47H_2O$ (**$Te_{15}Nb_{21}$**): $CuSO_4\cdot 5H_2O$ (1.997 g, 12.5 mmol) was dissolved in 5 mL distilled water under stirring followed by addition

of ethylenediamine (en) (5 mL). The resulting blue-violet solution was then added dropwise to a mixed solution containing $K_7HNb_6O_{19}\cdot13H_2O$ (1.7 g, 1.2 mmol) and Na_2TeO_3 (1.332 g, 6.0 mmol) in distilled water (130 mL). Next, the mixture was stirred for 13 h and adjusted to pH 10.5 using 6 mol L^{-1} HCl. Subsequently, the obtained mixture was heated at 90 °C for 5-6 h, and then cooled to room temperature and filtered. Purple block-shaped crystals were obtained within a week (yield 19 % based on Nb). IR (KBr disks): 3371, 3313, 3217, 1634, 1584, 1457, 1386, 1313, 1279, 1161, 1107, 1044, 983, 866, 717, 650, 525 cm^{-1}. Elemental analysis (%) calculated for $Te_{15}Nb_{21}Cu_{12}C_{36}N_{36}H_{253}O_{149}$: Nb, 23.78; Te, 23.33; Cu, 9.29; C, 5.27; N, 6.14; H, 3.10; found for: Nb, 23.57; Te, 23.05; Cu, 9.12; C, 5.03; N, 5.94; H, 2.93.

$[\{Cu(en)_2\}_6][Te_{10}Nb_{14}Na_2(OH)_2O_{61}]\cdot36H_2O$ (**$Te_{10}Nb_{14}$**): En was added dropwise to $CuSO_4\cdot5H_2O$ (4.52 g, 28.3 mmol) dissolved in 10 mL distilled water with stirring. The resulting blue-violet solution was then added dropwise to a solution of $K_7HNb_6O_{19}\cdot13H_2O$ (1.6 g, 1.2 mmol), Na_2TeO_3 (1.363 g, 6.1 mmol) and $Na_3PO_4\cdot12H_2O$ (2.6 mmol) in distilled water (130 mL). Next, the mixture was adjusted to pH 10.63 with 3 mol L^{-1} HCl solution and heated at 90 °C for 80 min and then cooled to room temperature. Purple block-shaped crystals obtained within a week (yield: 13 % based on Nb). IR (KBr disks): 3306, 3216, 2243, 1635, 1584, 1458, 1398, 1317, 1279, 1183, 1112, 1046, 982, 868, 705, 768, 526 cm^{-1}. Elemental analysis (%) calculated for $Na_2Te_{10}Nb_{14}O_{99}Cu_6C_{24}N_{24}H_{160}$: Nb, 24.19; Na, 0.85; Te, 23.73; Cu, 7.09; C, 5.36; N, 6.25; H, 3.07; found for: Nb, 24.51; Na, 0.62; Te, 24.03; Cu, 5.82; C, 4.37; N, 5.31; H, 2.70.

Typical procedure of the $Te_{15}Nb_{21}$ catalyzed amidation reactions. Succinic anhydride (0.5 mmol), phenylamine (0.5 mmol), DMSO (0.2 mL, if the reaction substrate is 1 mmol, the reaction can be solvent-free), **$Te_{15}Nb_{21}$** (1 mol%) were added in a 4-mL reaction vial. Then the reaction was carried out in screw cap vials with a Teflon seal at 140 °C for the desired time. After reaction, the mixture was purified by column chromatography (petroleum ether/EtOAc) to afford the desired products.

Characterization of $Te_{15}Nb_{21}$ and $Te_{10}Nb_{14}$.

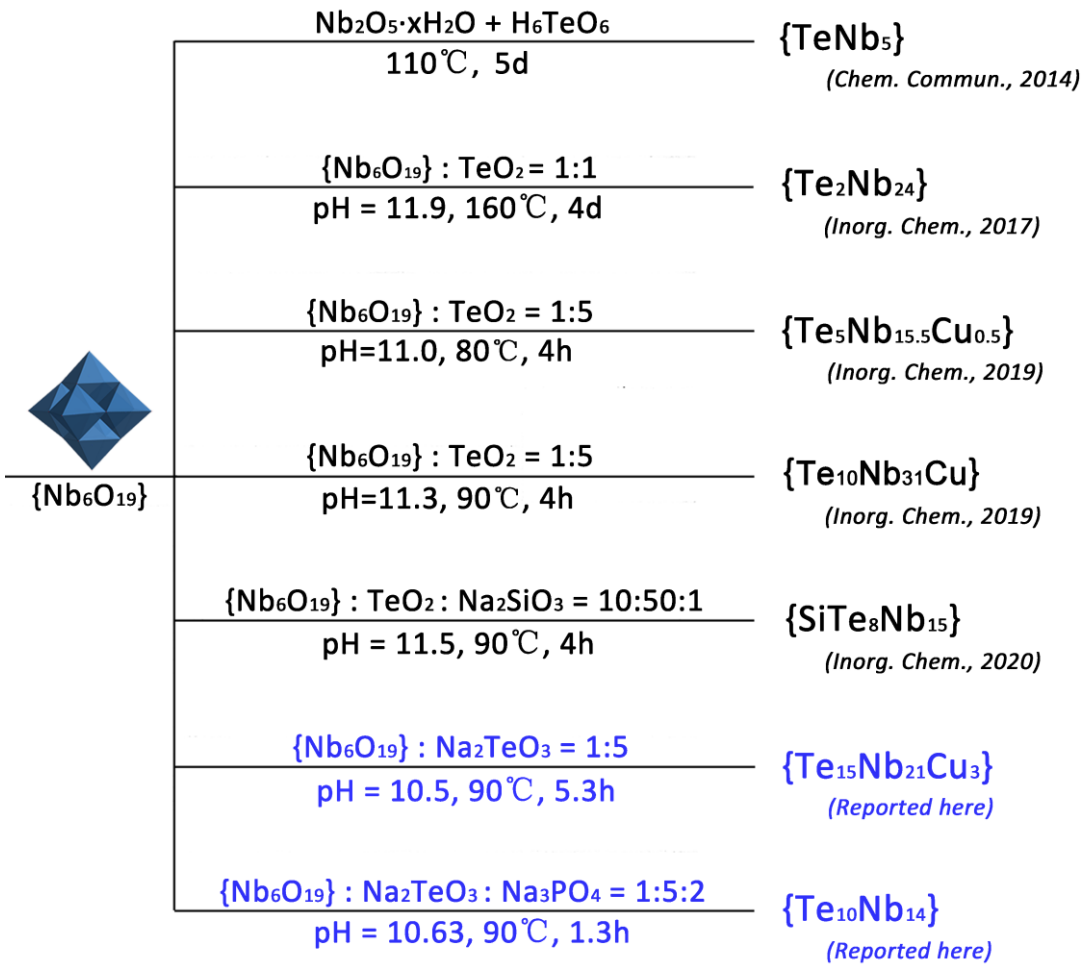

Scheme S1. Comparison of synthetic conditions of PONb clusters with Te as heteroatom.

Table S1. Crystal data and structure refinement of **$Te_{15}Nb_{21}$** and **$Te_{10}Nb_{14}$**.[S2-3]

Formula	**$Te_{15}Nb_{21}Cu_{12}C_{36}N_{36}H_{253}O_{149}$**	**$Na_2Te_{10}Nb_{14}O_{99}Cu_6C_{24}N_{24}H_{160}$**
Formula weight	8203	5374
Temperature/K	150	273.15
Crystal system	hexagonal	orthorhombic
Space group	$P6_3/m$	$C222_1$
a/Å	24.0801(4)	26.590(4)
b/Å	24.0801(4)	27.526(5)
c/Å	25.4757(4)	23.910(4)
α/°	90	90
β/°	90	90
γ/°	120	90
Volume/Å^3	12793.0(5)	17500(5)
Z	2	4
ρ_{calc}g/cm^3	2.311	1.769
μ/mm^{-1}	3.663	3.296
F(000)	6902.0	9048.0
Crystal size/mm^3	0.28 × 0.22 × 0.12	0.3 × 0.2 × 0.2
Radiation	MoKα (λ = 0.71073)	MoKα (λ = 0.71073)
2Θ range for data collection/°	4.656 to 56.564	4.26 to 50.054
Index ranges	-32 ≤ h ≤ 25, -32 ≤ k ≤ 32, -33 ≤ l ≤ 33	-31≤ h ≤ 31, -31 ≤ k ≤ 32, -28 ≤ l ≤ 28
Reflections collected	110906	53472
Independent reflections	10804 [R_{int} = 0.0484, R_{sigma} = 0.0235]	15185[R_{int} = 0.0567, R_{sigma} = 0.0599]
Data/restraints/parameters	10804/298/467	15185/405/682
Goodness-of-fit on F^2	1.042	1.068
Final R indexes [I>=2σ (I)]	R_1 = 0.0389, wR_2 = 0.1045	R_1 = 0.0502, wR_2 = 0.1315
Final R indexes [all data]	R_1 = 0.0484, wR_2 = 0.1121	R_1 = 0.0707, wR_2 = 0.1444

$^a R^1 = \sum||Fo|-|Fc||/\sum|Fo|$. $^b wR^2 = \{\sum[w(Fo^2-Fc^2)^2]/\sum[w(Fo^2)^2]\}^{1/2}$

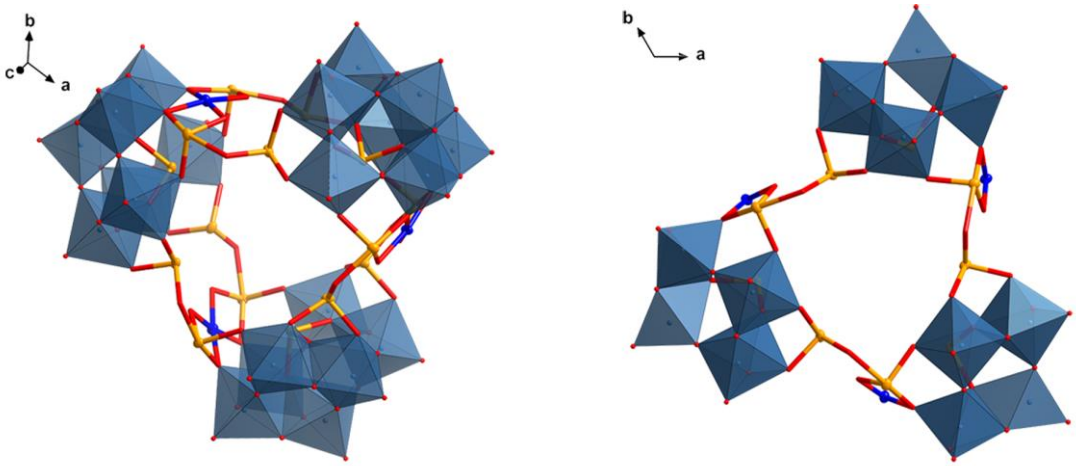

Figure S1. Combined polyhedral/ball-and-stick representation of the trimeric polyanion **$Te_{15}Nb_{21}$**, $[Te_{15}Nb_{21}Cu_3O_{96}]^{21-}$, highlighting the two different viewing directions. Color code: Te, orange; Nb, teal; Cu, blue; O, red.

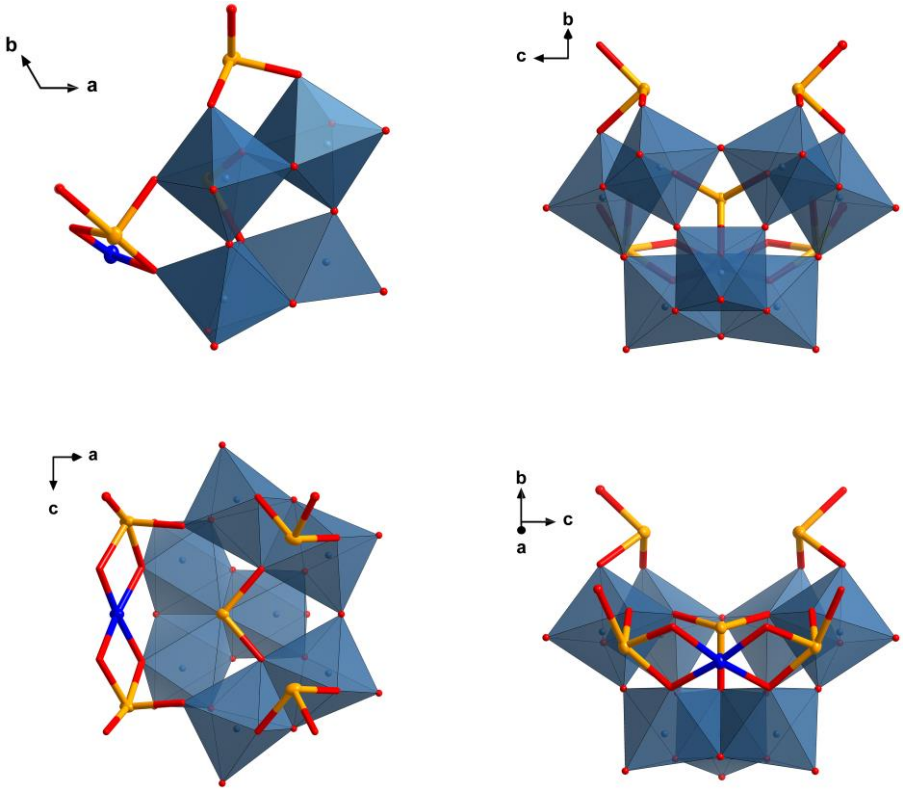

Figure S2. Combined polyhedral/ball-and-stick representation of $[Te_5Nb_7CuO_{34}]^{11-}$ subunit, highlighting the four different viewing directions. Color code: Te, orange; Nb, teal; Cu, blue; O, red.

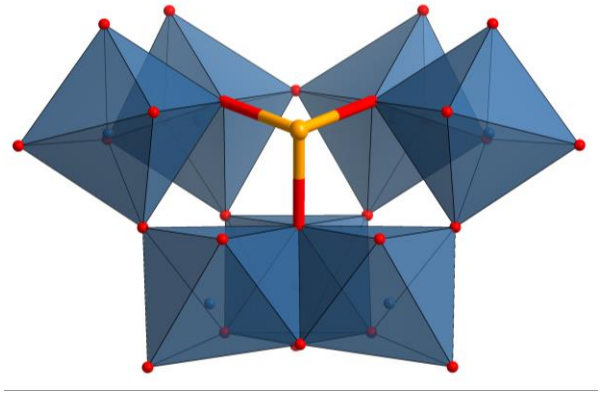

Figure S3. Combined polyhedral/ball-and-stick representation of $[TeNb_7O_{28}]^{17-}$ fragment, resulting from the the removal of one $\{Nb_3O_{13}\}$ triad and two $\{NbO_6\}$ octahedra of the other two $\{Nb_3O_{13}\}$ triads from the plenary Keggin cluster. Color code: Te, orange; Nb, teal; O, red.

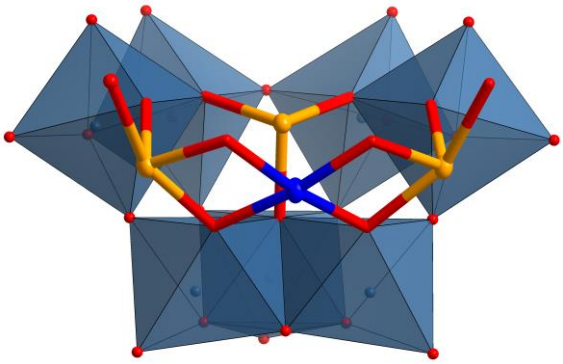

Figure S4. Combined polyhedral/ball-and-stick representation of polyanion $[Te\{Nb_7(Te_2Cu)\}O_{32}]^{15-}$, which can be regarded as a trivacant Keggin-type polyanion if the site of $\{Te_2Cu\}$ segment is replaced by two Nb centres. Color code: Te, orange; Nb, teal; Cu, blue; O, red.

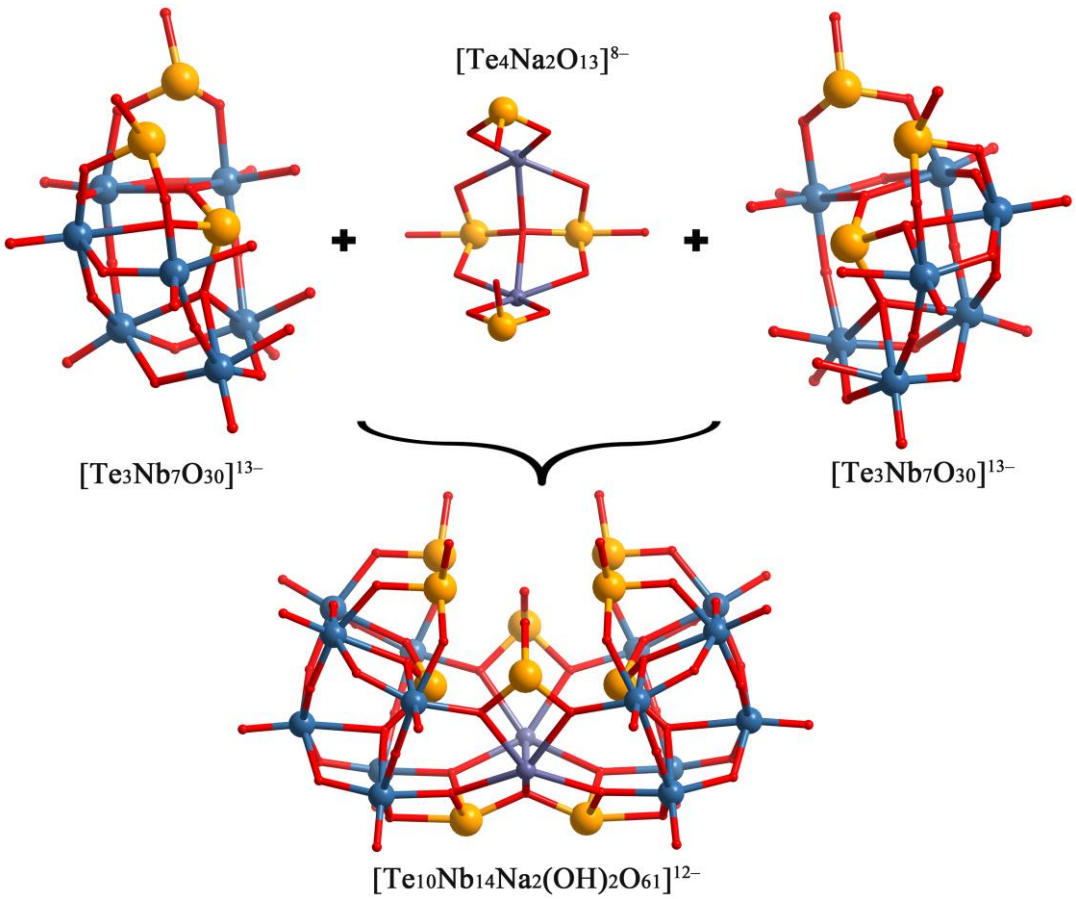

Figure S5. Schematic view of ball-and-stick representation of **$Te_{10}Nb_{14}$**, highlighting the sandwich-type dimer. Color code: Te, orange; Nb, teal; Na, blue gray; O, red.

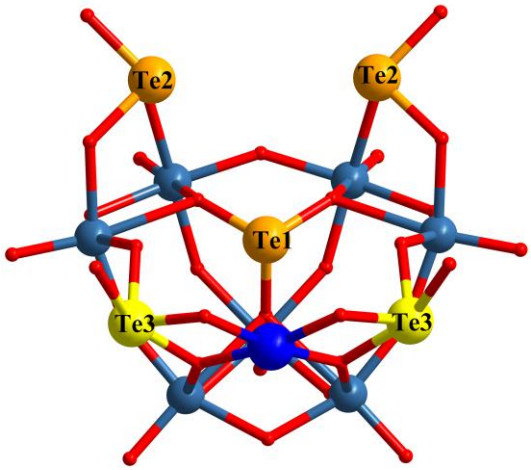

Figure S6. Ball-and-stick representation of $[Te_5Nb_7CuO_{34}]^{11-}$ subunit in **$Te_{15}Nb_{21}$**, highlighting the coordination environments of Te atoms, in which the tetra-coordinate and tri-coordinate tellurium atoms are shown in yellow and orange, respectively. Color code: Te, orange; Nb, teal; Cu, blue; O, red.

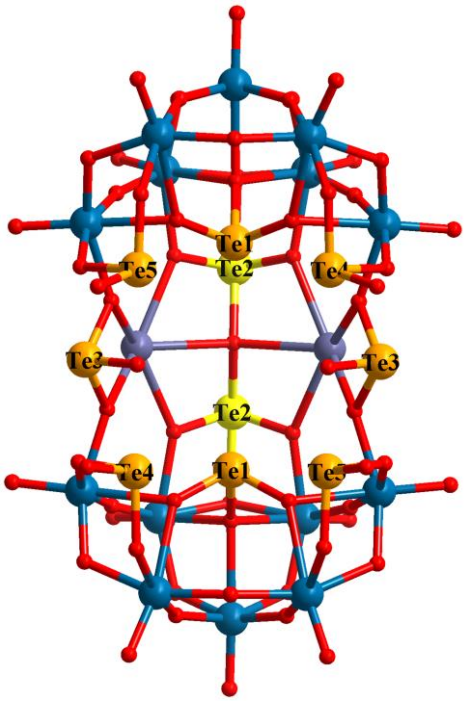

Figure S7. Ball-and-stick representation of polyanion **$Te_{10}Nb_{14}$**, highlighting the coordination environments of Te atoms, in which the tetra-coordinate and tri-coordinate tellurium atoms are shown in yellow and orange, respectively. Color code: Te, orange; Nb, teal; Na, blue gray; O, red.

Table S2. Bond valence sum calculations for Nb, Te, Cu and O atoms in **$Te_{15}Nb_{21}$**.

Atom	BVS	Atom	BVS	Atom	BVS
Te1	3.99	O2	1.93	O11	1.80
Te2	3.75	O3	1.69	O12	2.10
Te3	4.11	O4	1.90	O13	1.85
Nb1	4.97	O5	1.83	O14	1.82
Nb2	4.95	O6	1.86	O15	1.46
Nb3	4.92	O7	1.83	O16	1.42
Nb4	4.93	O8	1.69	O17	1.45
Cu1	2.04	O9	1.87	O18	1.51
O1	2.01	O10	1.72	O19	2.01

Table S3. Bond valence sum calculations for Nb, Te and O atoms in **$Te_{10}Nb_{14}$**.

Atom	BVS	Atom	BVS	Atom	BVS
Te1	3.90	O4	1.87	O19	1.47
Te2	4.21	O5	2.02	O20	1.42
Te3	4.06	O6	1.39	O21	1.83
Te4	3.63	O7	1.51	O22	1.77
Te5	3.87	O8	1.74	O23	1.89
Nb1	5.03	O9	1.55	O24	1.86
Nb2	4.93	O10	2.03	O25	1.58
Nb3	5.05	O11	1.95	O26	1.85
Nb4	5.13	O12	1.72	O27	1.71
Nb5	4.91	O13	1.95	O28	1.40
Nb6	5.22	O14	2.10	O29	1.19*
Nb7	5.04	O15	1.98	O30	1.77
O1	1.99	O16	1.55	O31	1.94
O2	1.81	O17	1.89	O32	1.72
O3	1.77	O18	1.82		

*Represents the monoprotonated oxygen atom.

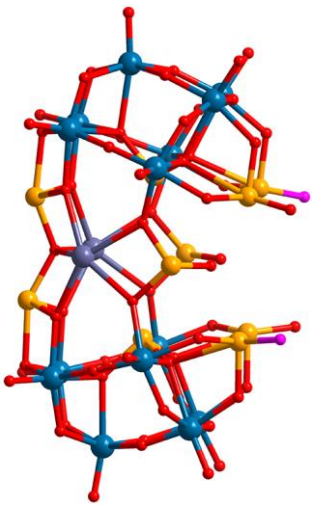

Figure S8. Ball-and-stick representation of polyanion **$Te_{10}Nb_{14}$**, highlighting the protonated oxygen atoms, O and OH ligands are shown in red and pink, respectively. Color code: Te, orange; Nb, teal; Na, blue gray; O, red.

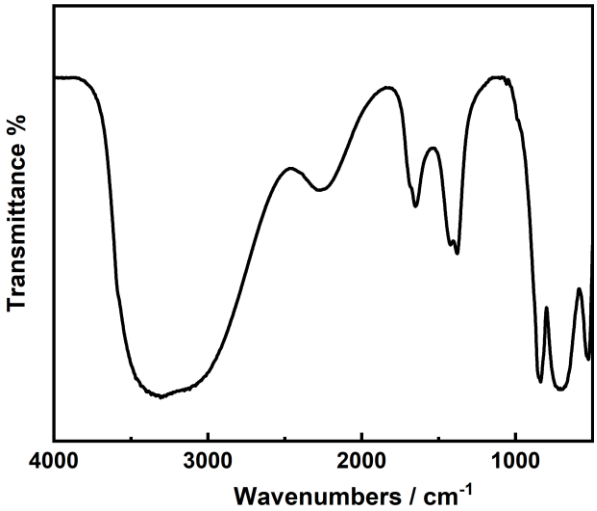

Figure S9. The IR spectrum of $K_7HNb_6O_{19}\cdot 13H_2O$ (Nb_6O_{19}) in the range of 4000-500 cm^{-1}.

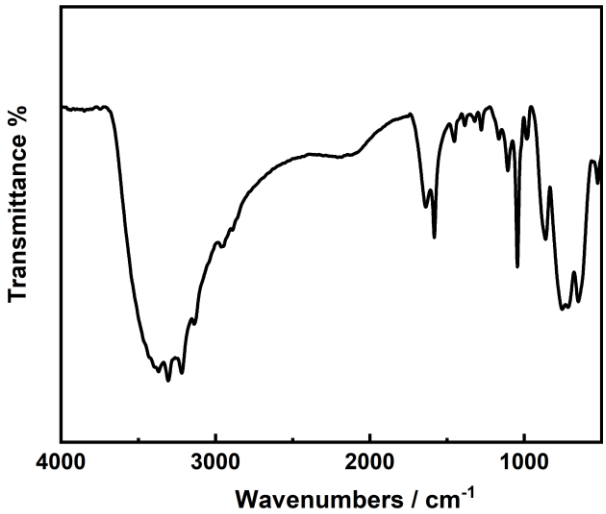

Figure S10. The IR spectrum of $\mathbf{Te_{15}Nb_{21}}$ in the range of 4000-500 cm^{-1}.

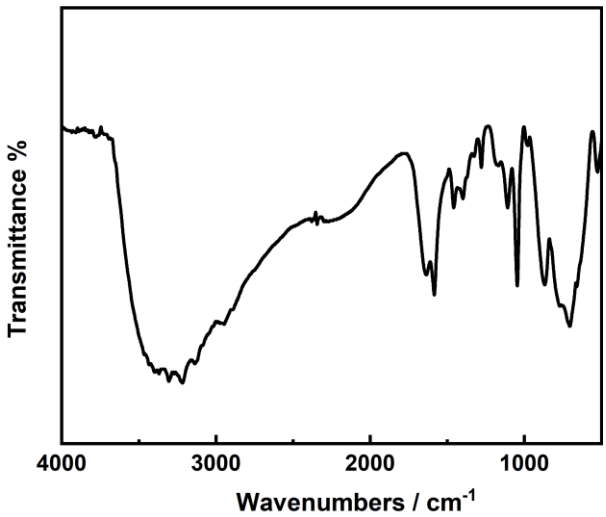

Figure S11. The IR spectrum of $\mathbf{Te_{10}Nb_{14}}$ in the range of 4000-500 cm^{-1}.

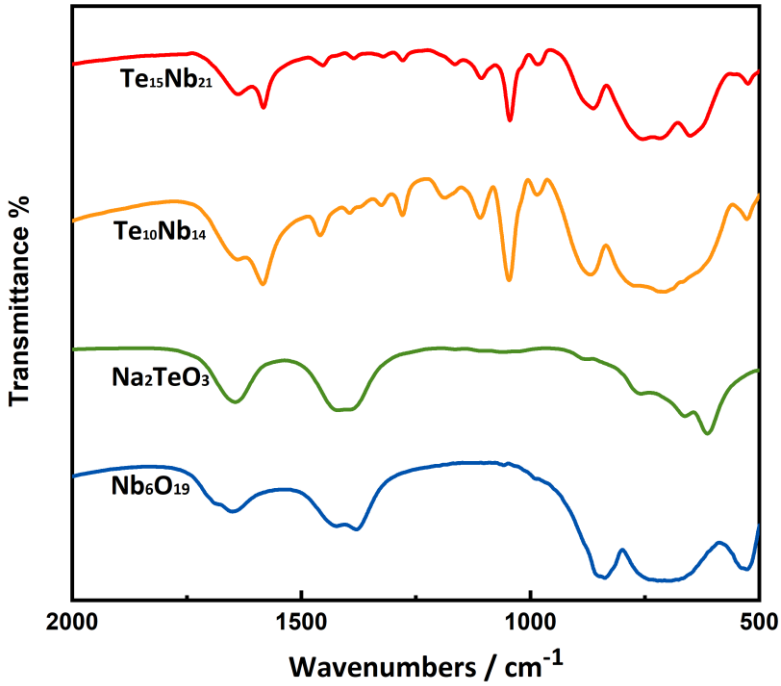

Figure S12. IR spectra for Nb_6O_{19}, Na_2TeO_3, **$Te_{15}Nb_{21}$** and **$Te_{10}Nb_{14}$** in the region of 500-2000 cm^{-1}.

As shown in Figures S9-12, the Fourier transform infrared (FTIR) spectra of **$Te_{15}Nb_{21}$** and **$Te_{10}Nb_{14}$** are nearly identical, being characterized by absorptions in the region 500-900 cm^{-1}, attributed to metal-oxygen vibrations, and in the regions 1600-1650 and 2800-4000 cm^{-1}, assigned to water of crystallization. The characteristic vibration of Te-O appears at ca. 650 cm^{-1}, whereas the band at ca. 1045 cm^{-1} is attributed to en. Compared with the IR spectrum of $K_7HNb_6O_{19}\cdot 13H_2O$ (Nb_6O_{19}), the band at ca. 860 cm^{-1} for the Nb-O_t stretching vibration enhances obviously because of the coordination of Te atoms to Nb_6O_{19} fragments.

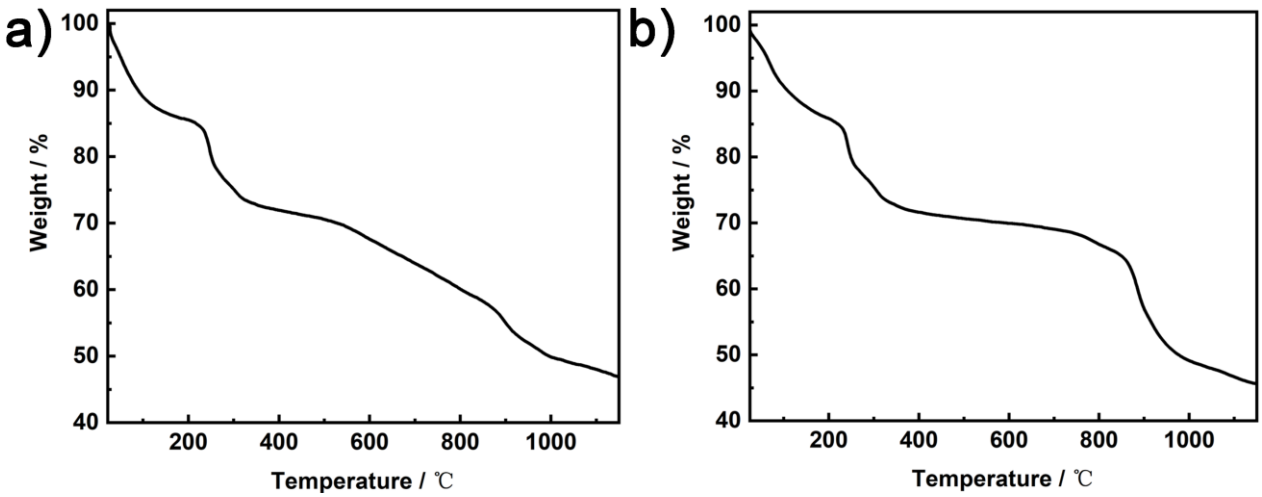

Figure S13. The TG curve of **$Te_{15}Nb_{21}$** (a) and **$Te_{10}Nb_{14}$** (b).

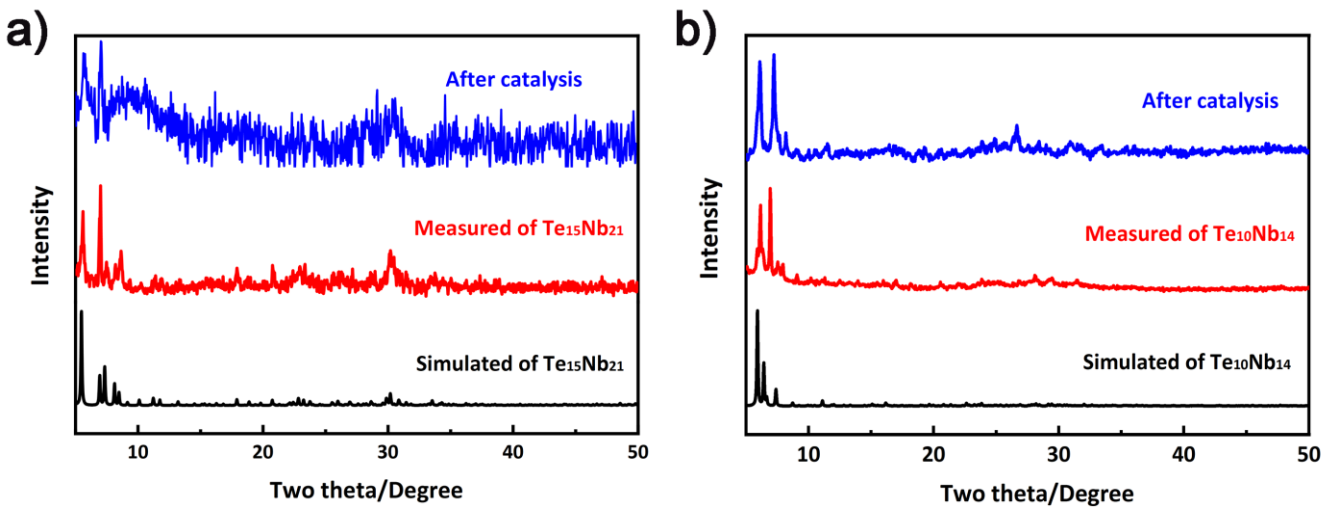

Figure S14. Simulated (black), measured (red) and after catalysis (blue) powder X-ray diffraction patterns of **$Te_{15}Nb_{21}$** (a) and **$Te_{10}Nb_{14}$** (b).

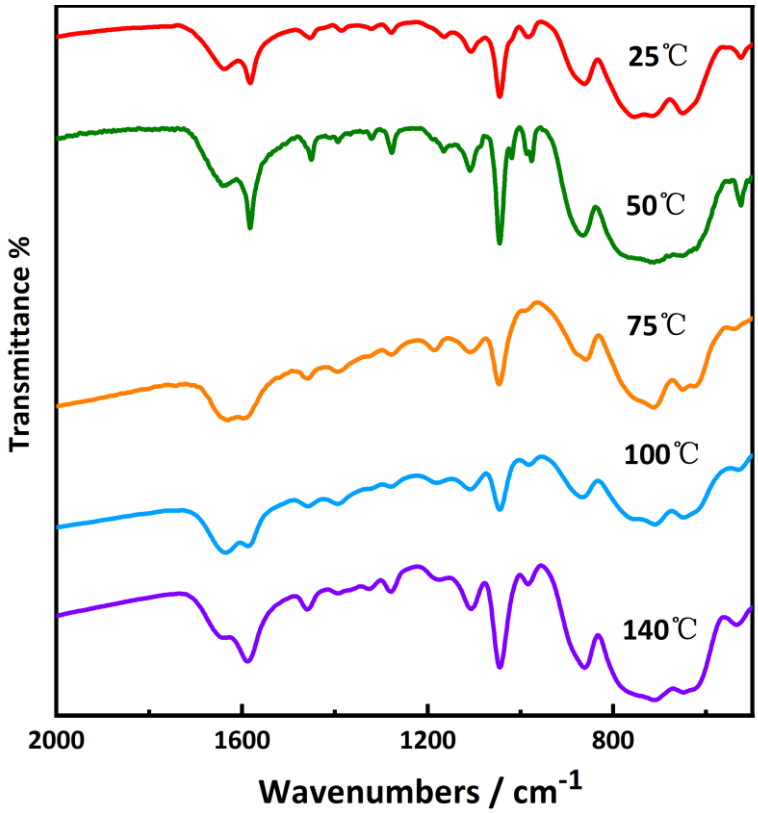

Figure S15. Variable temperature IR spectra of **$Te_{15}Nb_{21}$**.

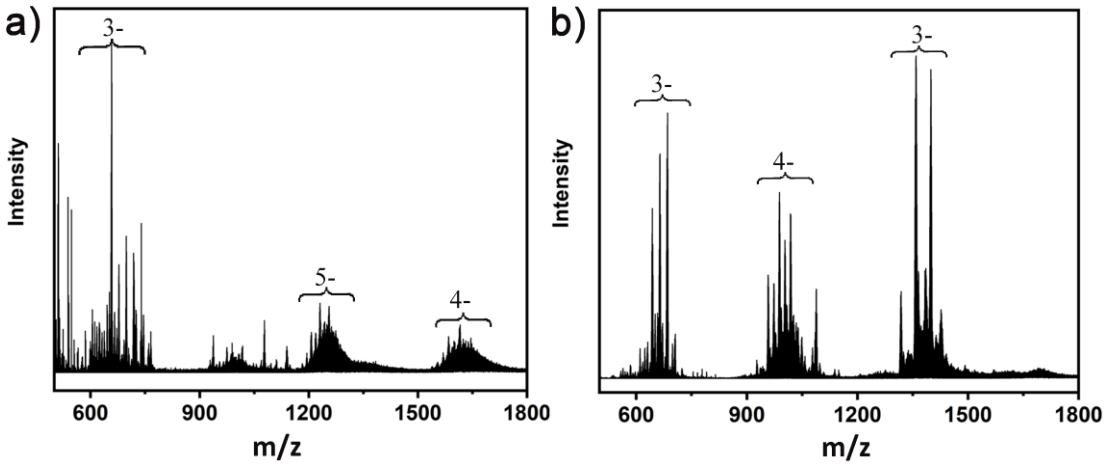

Figure S16. The negative-ion ESI mass spectrum of cluster anion in **$Te_{15}Nb_{21}$** and **$Te_{10}Nb_{14}$**.

$Te_{15}Nb_{21}$, **$Te_{10}Nb_{14}$** were dissolved in high-purity water and their solution behaviors were detected by ESI-MS. The peak envelopes are broad due to association of a range of counterions and solvent molecules, which is typical in ESI-MS of larger POMs. For **$Te_{15}Nb_{21}$**, all the major peaks in the spectrum could be assigned to the formula $[Te_{15}Nb_{21}Cu_3O_{96}]^{21-}$ (Tables S4). The charge of the envelopes in the range of m/z 1550-1700 and 1200-1300 is 4- and 5-, respectively (Figure S16a). For polyanion **$Te_{10}Nb_{14}$**, similar patterns were also detected for the 3- and 4-, and charge envelopes in the range of *m/z* 1300-1450 and 950-1100 is 4- and 5-, respectively (Figure S16b and Table S5).

Table S4. Assignment of peaks of **$Te_{15}Nb_{21}$.**

Entry	Identification	Charge	m / z (calcd)	m / z (found)
1	$\{Te_{15}Nb_{21}Cu_3O_{96}Cu_5(C_2N_2H_8)_9(H_2O)_7H_7\}$	-4	1645.84	1645.91
2	$\{Te_{15}Nb_{21}Cu_3O_{96}Cu_4(C_2N_2H_8)_4(H_2O)_{24}H_9\}$	-4	1631.91	1631.92
3	$\{Te_{15}Nb_{21}Cu_3O_{96}Cu_4(C_2N_2H_8)_8(H_2O)_7H_9\}$	-4	1615.44	1615.40
4	$\{Te_{15}Nb_{21}Cu_3O_{96}Cu_3(C_2N_2H_8)_4(H_2O)_{17}H_{11}\}$	-4	1585.00	1585.15
5	$\{Te_{15}Nb_{21}Cu_3O_{96}Cu_2(C_2N_2H_8)_4(H_2O)_{17}H_{12}\}$	-5	1255.49	1255.31
6	$\{Te_{15}Nb_{21}Cu_3O_{96}Cu(C_2N_2H_8)_2(H_2O)_{20}H_{14}\}$	-5	1229.95	1230.10
7	$\{Te_{15}Nb_{21}Cu_3O_{96}Cu_2(C_2N_2H_8)_4(H_2O)_7H_{12}\}$	-5	1219.46	1219.69
8	$\{Te_{15}Nb_{21}Cu_3O_{96}Cu(C_2N_2H_8)(H_2O)_{17}H_{14}\}$	-5	1207.13	1207.10

Table S5. Assignment of peaks of **$Te_{10}Nb_{14}$.**

Entry	Identification	Charge	m / z (calcd)	m / z (found)
1	$\{Te_{10}Nb_{14}Na_5O_{63}Cu_2(C_2N_2H_8)_3(H_2O)_{15}H_4\}$	-3	1427.08	1427.26
2	$\{Te_{10}Nb_{14}Na_2O_{63}Cu_2(C_2N_2H_8)_4(H_2O)_{11}H_7\}$	-3	1401.11	1401.24
3	$\{Te_{10}Nb_{14}Na_2O_{63}Cu_2(C_2N_2H_8)_3(H_2O)_{14}H_7\}$	-3	1399.10	1399.24
4	$\{Te_{10}Nb_{14}Na_2O_{63}Cu_2(C_2N_2H_8)_4(H_2O)_4H_7\}$	-3	1359.08	1358.92
5	$\{Te_{10}Nb_{14}Na_3O_{63}Cu(C_2N_2H_8)_2(H_2O)_6H_9\}$	-3	1318.18	1318.24
6	$\{Te_{10}Nb_{14}Na_2O_{63}Cu_2(C_2N_2H_8)_3(H_2O)_{14}H_6\}$	-4	1049.07	1049.17
7	$\{Te_{10}Nb_{14}Na_3O_{63}Cu_2(C_2N_2H_8)_3(H_2O)_6H_5\}$	-4	1018.54	1018.42
8	$\{Te_{10}Nb_{14}Na_3O_{63}Cu_2(C_2N_2H_8)_2(H_2O)_6H_5\}$	-4	1003.51	1003.40
9	$\{Te_{10}Nb_{14}Na_2O_{63}Cu_2(C_2N_2H_8)_2(H_2O)_7H_6\}$	-4	1002.52	1002.40
10	$\{Te_{10}Nb_{14}Na_4O_{63}Cu(C_2N_2H_8)(H_2O)_8H_6\}$	-4	987.61	987.67

Optimization of reaction conditions

Table S6. Condition optimization for the amidation reaction.[a]

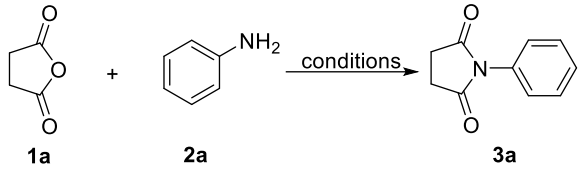

Entry	Catalyst (mol%)	Temp. (°C)	Time (h)	Yield[b] (%)
1	**$Te_{15}Nb_{21}$** (1.0)	100	5	23
2	**$Te_{10}Nb_{14}$** (1.5)	100	5	19
3	**$Te_{15}Nb_{21}$** (1.0)	120	5	58
4	**$Te_{15}Nb_{21}$** (1.0)	140	5	65
5	**$Te_{15}Nb_{21}$** (1.0)	140	8	70
6	**$Te_{15}Nb_{21}$** (1.0)	140	10	78
7	**$Te_{15}Nb_{21}$** (1.0)	140	12	94

[a] Reaction conditions: succinic anhydride **1a** (0.5 mmol), phenylamine **2a** (0.5 mmol), DMSO (0.2 mL). [b] The yields were determined by GC with biphenyl as the internal standard; N.D. = no detected.

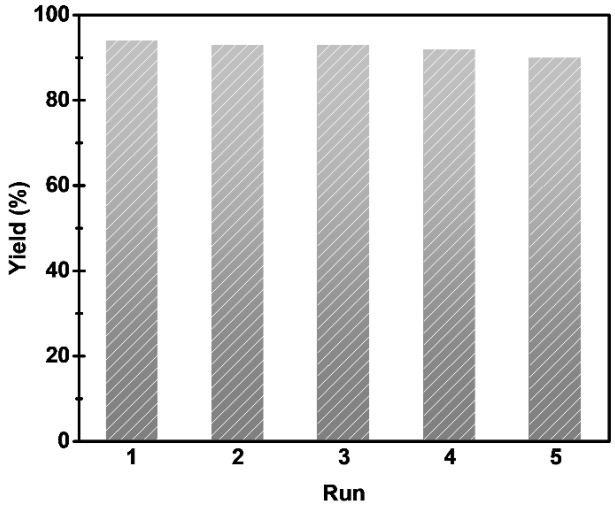

Figure S17. Recyclability of catalyst **$Te_{15}Nb_{21}$.**

Characterization of substrates and products

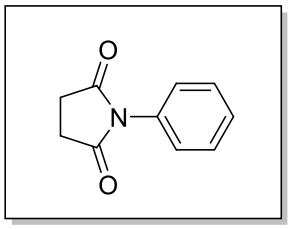

1-phenylpyrrolidine-2,5-dione (3a)[S3]

^{1}H NMR (500 MHz, $CDCl_3$) δ 7.48 (t, *J* = 7.7 Hz, 2H), 7.40 (t, *J* = 7.5 Hz, 1H), 7.27 (d, *J* = 7.4 Hz, 2H), 2.85 (s, 4H);

^{13}C NMR (126 MHz, $CDCl_3$) δ = 176.35, 131.93, 129.24, 128.69, 126.52, 28.63.

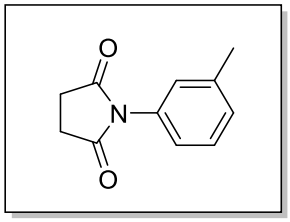

1-(m-tolyl)pyrrolidine-2,5-dione (3b)[S3]

^{1}H NMR (500 MHz, $CDCl_3$) δ 7.34 (t, *J* = 7.7 Hz, 1H), 7.19 (d, *J* = 7.6 Hz, 1H), 7.13-6.97 (m, 2H), 2.80 (s, 4H), 2.37 (s, 3H);

^{13}C NMR (126 MHz, $CDCl_3$) δ = 176.50, 139.29, 131.86, 129.57, 129.06, 127.17, 123.65, 28.44, 21.38.

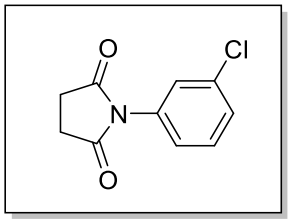

1-(3-chlorophenyl)pyrrolidine-2,5-dione (3c)[S3]

^{1}H NMR (500 MHz, $CDCl_3$) δ 7.40-7.34 (m, 2H), 7.31 (s, 1H), 7.17 (d, *J* = 7.3 Hz, 1H), 2.80 (s, 4H);

^{13}C NMR (126 MHz, $CDCl_3$) δ = 175.95, 134.52, 133.07, 130.19, 128.76, 126.73, 124.76, 28.37.

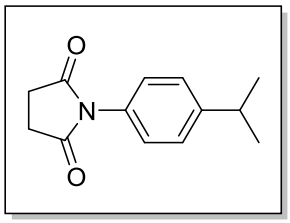

1-(4-isopropylphenyl)pyrrolidine-2,5-dione (3d)[S3]

^{1}H NMR (500 MHz, $CDCl_3$) δ 7.32 (d, *J* = 8.0 Hz, 2H), 7.17 (d, *J* = 8.0 Hz, 2H), 2.93 (dt, *J* = 13.7, 6.8 Hz, 1H), 2.82 (s, 4H), 1.25 (d, *J* = 7.0 Hz, 6H);

^{13}C NMR (126 MHz, $CDCl_3$) δ = 176.56, 149.41, 129.48, 127.33, 126.32, 33.92, 28.41, 23.92.

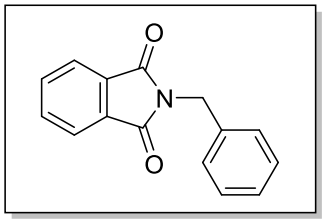

2-benzylisoindoline-1,3-dione (3e)[S4]

^{1}H NMR (500 MHz, $CDCl_3$) δ 7.69 (dd, *J* = 5.3, 3.1 Hz, 2H), 7.53 (dd, *J* = 5.4, 3.1 Hz, 2H), 7.31 (d, *J* = 7.3 Hz, 2H), 7.19 (t, *J* = 7.4 Hz, 2H), 7.13 (t, *J* = 7.3 Hz, 1H), 4.71 (s, 2H);

^{13}C NMR (126 MHz, $CDCl_3$) δ = 168.02, 136.43, 134.00, 132.08, 128.71, 128.65, 127.86, 123.33, 41.60.

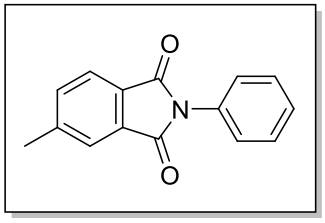

5-methyl-2-phenylisoindoline-1,3-dione (3f)[S5]

^{1}H NMR (500 MHz, $(CD_3)_2SO$) δ 7.79 (d, *J* = 7.6 Hz, 1H), 7.74 (s, 1H), 7.65 (d, *J* = 7.6 Hz, 1H), 7.48-7.45 (m, 2H), 7.38 (dd, *J* = 7.6, 4.4 Hz, 3H), 2.46 (s, 3H);

^{13}C NMR (126 MHz, $(CD_3)_2SO$) δ = 167.56, 167.46, 146.17, 135.55, 132.42, 132.35, 129.38, 129.31, 128.46, 127.83, 124.31, 123.84, 21.89.

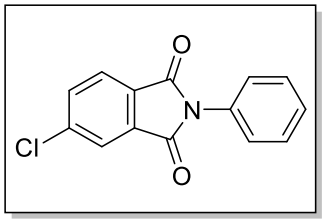

5-chloro-2-phenylisoindoline-1,3-dione (3g)[S5]

^{1}H NMR (500 MHz, $CDCl_3$) δ 7.83 (d, *J* = 1.7 Hz, 1H), 7.80 (d, *J* = 8.0 Hz, 1H), 7.66 (dd, *J* = 8.0, 1.8 Hz, 1H), 7.45-7.41 (m, 2H), 7.34 (dd, *J* = 6.7, 2.2 Hz, 3H);

^{13}C NMR (126 MHz, $CDCl_3$) δ = 166.35, 166.04, 141.14, 134.53, 133.41, 131.40, 129.80, 129.22, 128.35, 126.50, 125.06, 124.20.

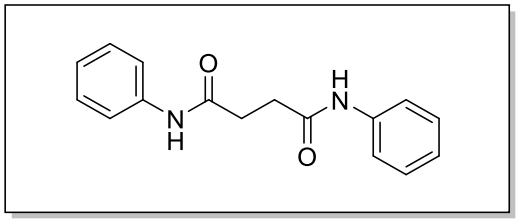

***N*^{1}, *N*^{4}-diphenylsuccinamide (4a)[S6]**

^{1}H NMR (500 MHz, $(CD_3)_2SO$) δ 9.89 (s, 2H), 7.47 (d, *J* = 8.0 Hz, 4H), 7.14 (t, *J* = 7.8 Hz, 4H), 6.88 (t, *J* = 7.3 Hz, 2H), 2.54 (s, 4H);

^{13}C NMR (126 MHz, $(CD_3)_2SO$) δ = 170.87, 139.81, 129.14, 123.37, 119.36, 31.66.

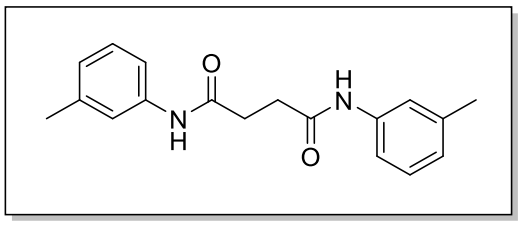

***N*^{1}, *N*^{4}-di-m-tolylsuccinamide (4b)**

^{1}H NMR (500 MHz, $(CD_3)_2SO$) δ 9.81 (s, 2H), 7.34 (s, 2H), 7.26 (d, *J* = 8.2 Hz, 2H), 7.03 (t, *J* = 7.8 Hz, 2H), 6.71 (d, *J* = 7.5 Hz, 2H), 2.53 (s, 4H), 2.13 (s, 6H);

^{13}C NMR (126 MHz, $(CD_3)_2SO$) δ = 170.79, 139.75, 138.27, 128.96, 124.06, 119.91, 116.58, 31.70, 21.68.

HRMS (ESI): m/z, calcd. for $C_{18}H_{21}N_2O_2$ $[M+H]^+$ requires 297.1598, found 297.1601.

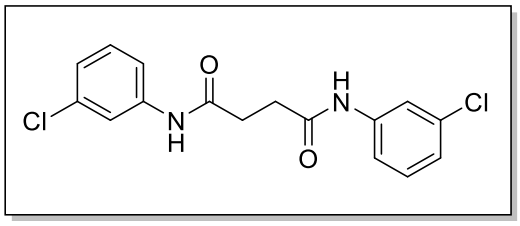

***N*^{1}, *N*^{4}-bis(3-chlorophenyl)succinamide (4c)**

^{1}H NMR (500 MHz, $(CD_3)_2SO$) δ 10.10 (s, 2H), 7.71 (s, 2H), 7.31 (d, *J* = 8.2 Hz, 2H), 7.18 (t, *J* = 8.1 Hz, 2H), 6.95 (d, *J* = 7.9 Hz, 2H), 2.55 (s, 4H);

^{13}C NMR (126 MHz, $(CD_3)_2SO$) δ = 171.21, 141.17, 133.53, 130.84, 123.09, 118.81, 117.69, 31.48.

HRMS (ESI): m/z, calcd. for $C_{16}H_{15}Cl_2N_2O_2$ $[M+H]^+$ requires 337.0505, found 337.0509.

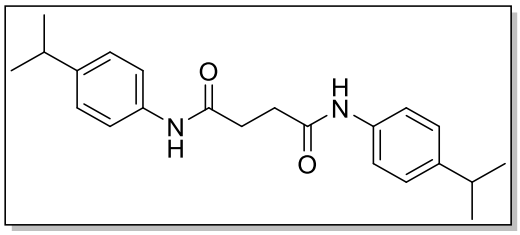

***N*^{1}, *N*^{4}-bis(4-isopropylphenyl)succinamide (4d)**

^{1}H NMR (500 MHz, $(CD_3)_2SO$) δ 9.82 (s, 2H), 7.40 (d, *J* = 8.5 Hz, 4H), 7.04 (d, *J* = 8.5 Hz, 4H), 2.76-2.65 (m, 2H) 2.53 (s, 4H), 1.06 (d, *J* = 6.9 Hz, 12H);

^{13}C NMR (126 MHz, $(CD_3)_2SO$) δ = 170.60, 143.37, 137.58, 126.80, 119.47, 33.31, 31.70, 24.44.

HRMS (ESI): m/z, calcd. for $C_{22}H_{29}N_2O_2$ $[M+H]^+$ requires 353.2224, found 353.2222.

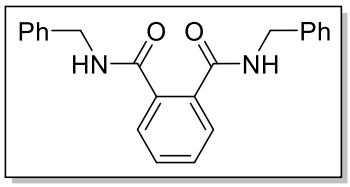

***N*[1], *N*[2]-dibenzylphthalamide (4e)[S7]**

^{1}H NMR (500 MHz, $(CD_3)_2SO$) δ 8.78 (t, *J* = 5.9 Hz, 2H), 7.47-7.41 (m, 4H), 7.31 (d, *J* = 7.5 Hz, 4H), 7.26 (t, *J* = 7.5 Hz, 4H), 7.17 (t, *J* = 7.2 Hz, 2H), 4.36 (d, *J* = 5.9 Hz, 4H);

^{13}C NMR (126 MHz, $(CD_3)_2SO$) δ = 168.69, 139.97, 136.83, 129.88, 128.70, 128.14, 127.66, 127.15, 42.91.

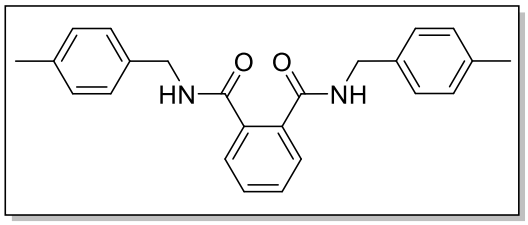

***N*[1], *N*[2]-bis(4-methylbenzyl)phthalamide (4f)**

^{1}H NMR (500 MHz, $(CD_3)_2SO$) δ 8.72 (t, *J* = 6.0 Hz, 2H), 7.45-7.40 (m, 4H), 7.19 (d, *J* = 7.9 Hz, 4H), 7.06 (d, *J* = 7.9 Hz, 4H), 4.30 (d, *J* = 6.0 Hz, 4H), 2.21 (s, 6H);

^{13}C NMR (126 MHz, $(CD_3)_2SO$) δ = 168.61, 136.91, 136.80, 136.13, 129.83, 129.24, 128.15, 127.66, 42.68, 21.17.

HRMS (ESI): m/z, calcd. for $C_{24}H_{25}N_2O_2$ $[M+H]^+$ requires 373.1911, found 373.1913.

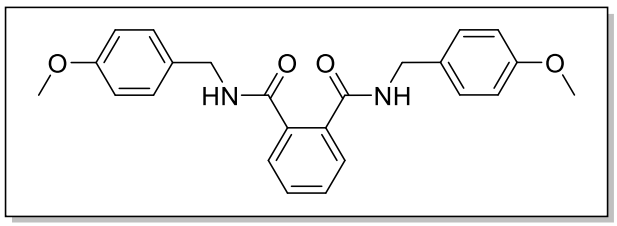

***N*[1], *N*[2]-bis(4-methoxybenzyl)phthalamide (4g)**

^{1}H NMR (500 MHz, $(CD_3)_2SO$) δ 8.63 (t, *J* = 5.9 Hz, 2H), 7.37-7.30 (m, 4H), 7.15 (d, *J* = 8.6 Hz, 4H), 6.73 (d, *J* = 8.6 Hz, 4H), 4.22 (d, *J* = 5.9 Hz, 4H), 3.56 (s, 6H);

^{13}C NMR (126 MHz, $(CD_3)_2SO$) δ = 168.65, 158.65, 136.80, 131.87, 129.85, 129.03, 128.18, 114.10, 55.49, 42.45.

HRMS (ESI): m/z, calcd. for $C_{24}H_{25}N_2O_4$ $[M+H]^+$ requires 405.1809, found 405.1806.

NMR Spectra

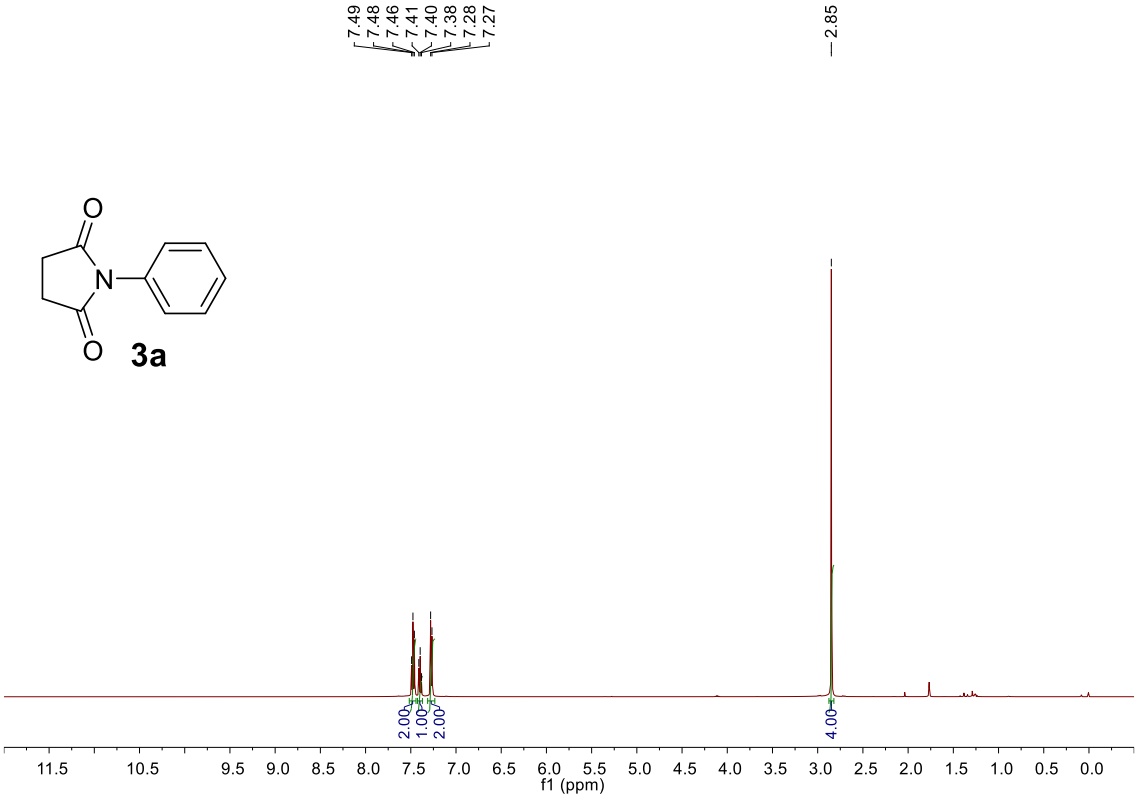
7.49
7.48
7.46
7.41
7.40
7.38
7.28
7.27
2.85
3a
2.00
1.00
2.00
4.00
11.5 10.5 9.5 9.0 8.5 8.0 7.5 7.0 6.5 6.0 5.5 5.0 4.5 4.0 3.5 3.0 2.5 2.0 1.5 1.0 0.5 0.0
f1 (ppm)

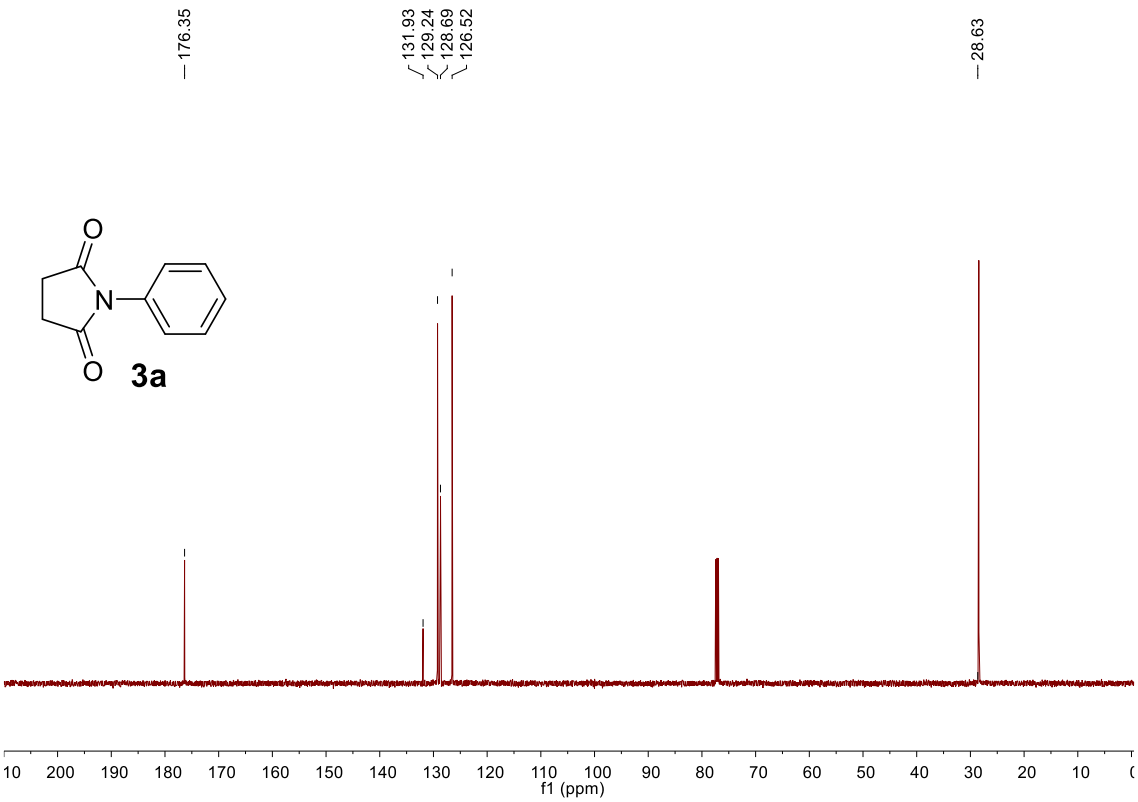
176.35
131.93
129.24
128.69
126.52
28.63
3a
10 200 190 180 170 160 150 140 130 120 110 100 90 80 70 60 50 40 30 20 10
f1 (ppm)

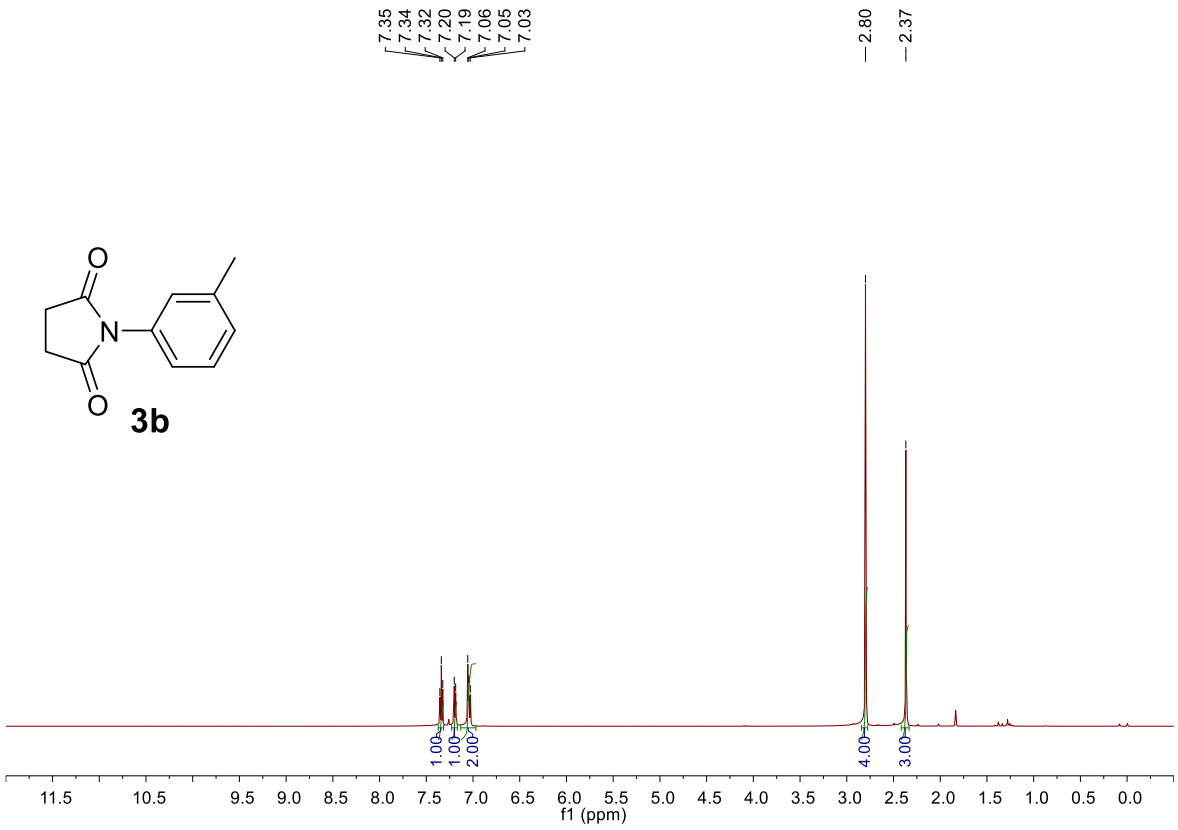
7.35
7.34
7.32
7.20
7.19
7.06
7.05
7.03
2.80
2.37
3b
1.00
1.00
2.00
4.00
3.00
f1 (ppm)

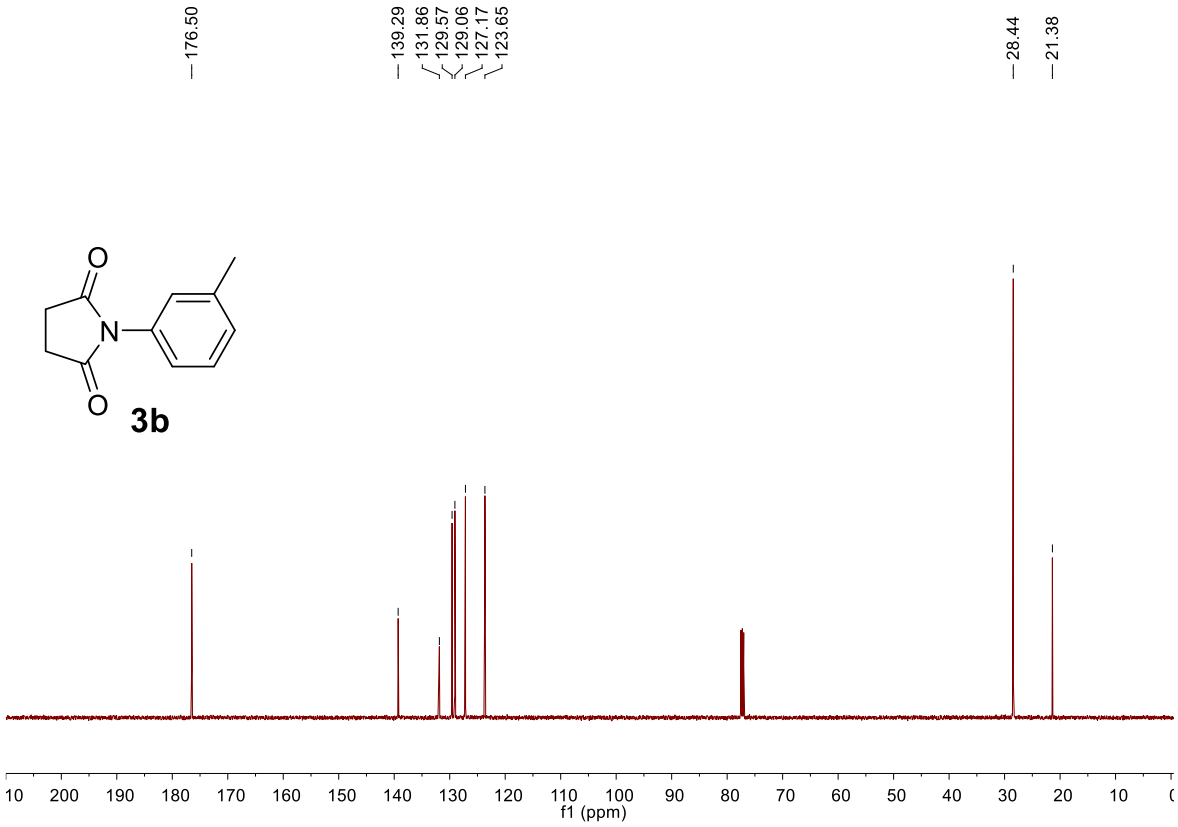
176.50
139.29
131.86
129.57
129.06
127.17
123.65
28.44
21.38
3b
f1 (ppm)

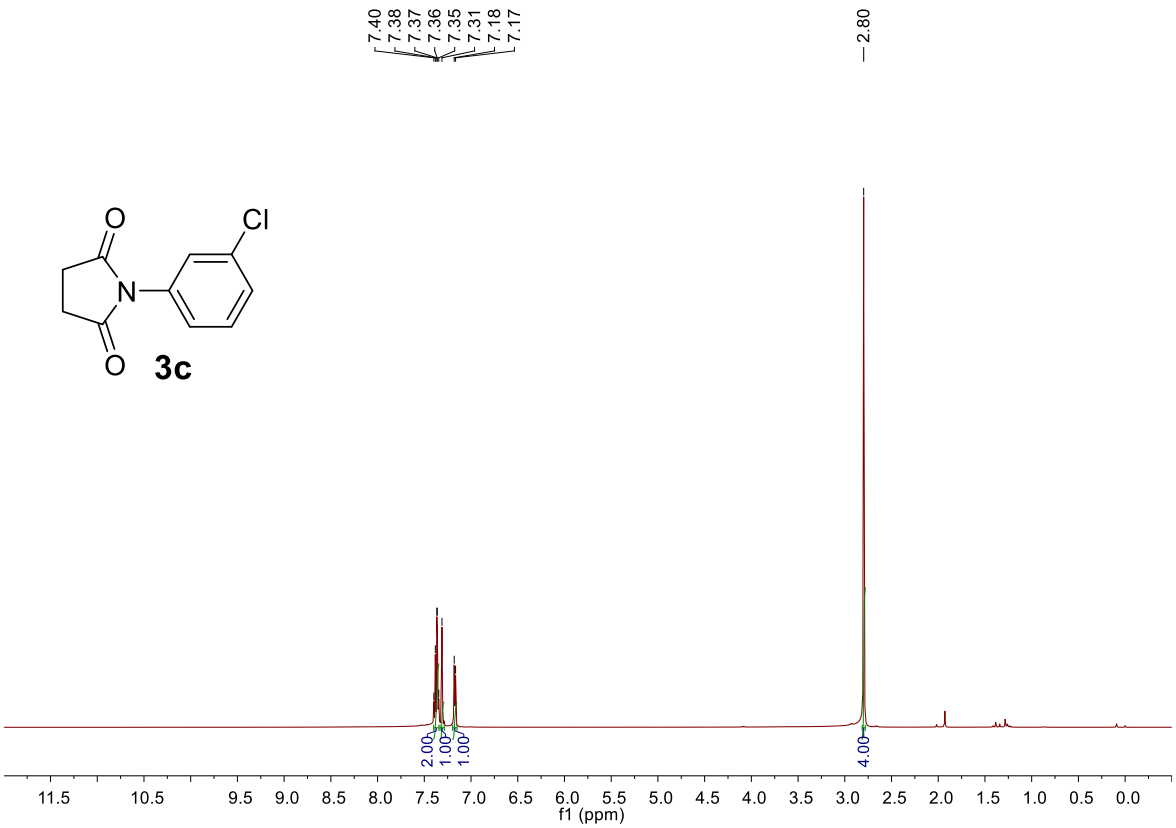
7.40
7.38
7.37
7.36
7.35
7.31
7.18
7.17
2.80
O
Cl
N
O
3c
2.00
1.00
1.00
4.00
11.5 10.5 9.5 9.0 8.5 8.0 7.5 7.0 6.5 6.0 5.5 5.0 4.5 4.0 3.5 3.0 2.5 2.0 1.5 1.0 0.5 0.0
f1 (ppm)

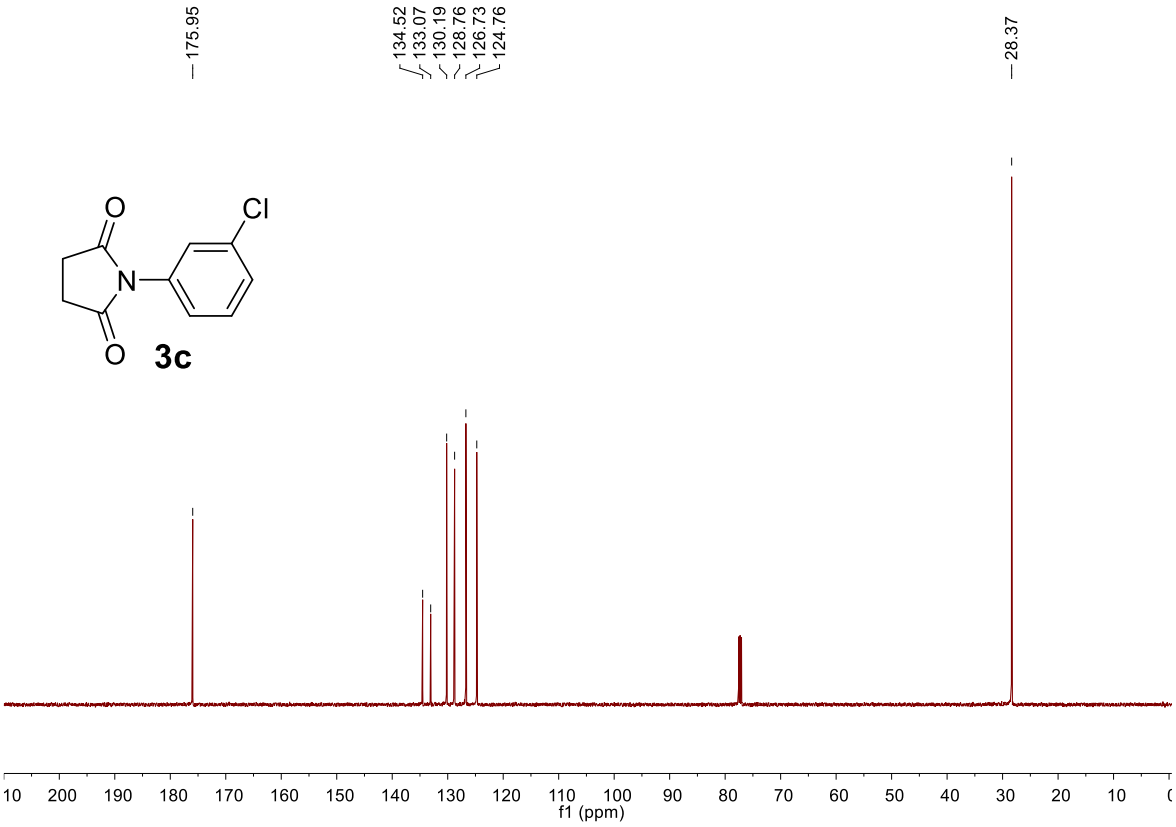
175.95
134.52
133.07
130.19
128.76
126.73
124.76
28.37
O
Cl
N
O
3c
10 200 190 180 170 160 150 140 130 120 110 100 90 80 70 60 50 40 30 20 10
f1 (ppm)

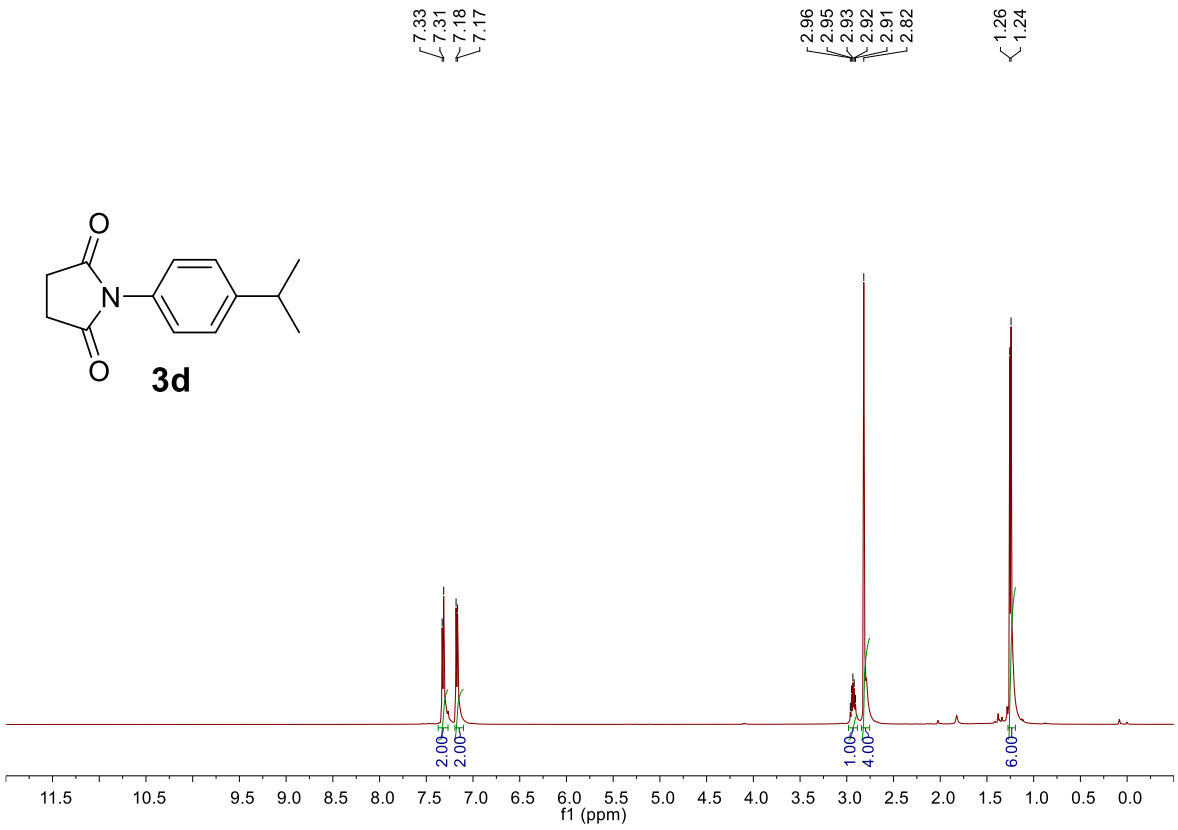
7.33
7.31
7.18
7.17
2.96
2.95
2.93
2.92
2.91
2.82
1.26
1.24
3d
2.00
2.00
1.00
4.00
6.00
11.5 10.5 9.5 9.0 8.5 8.0 7.5 7.0 6.5 6.0 5.5 5.0 4.5 4.0 3.5 3.0 2.5 2.0 1.5 1.0 0.5 0.0
f1 (ppm)

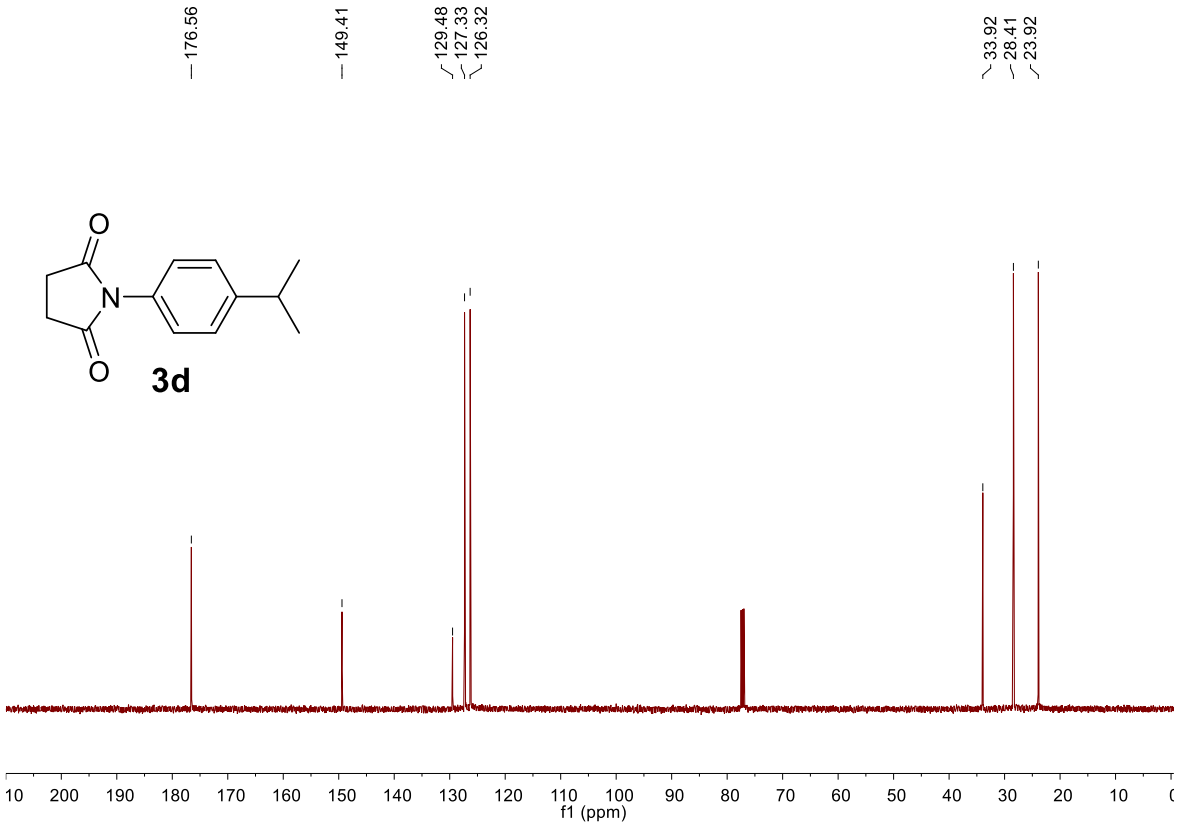
176.56
149.41
129.48
127.33
126.32
33.92
28.41
23.92
3d
10 200 190 180 170 160 150 140 130 120 110 100 90 80 70 60 50 40 30 20 10
f1 (ppm)

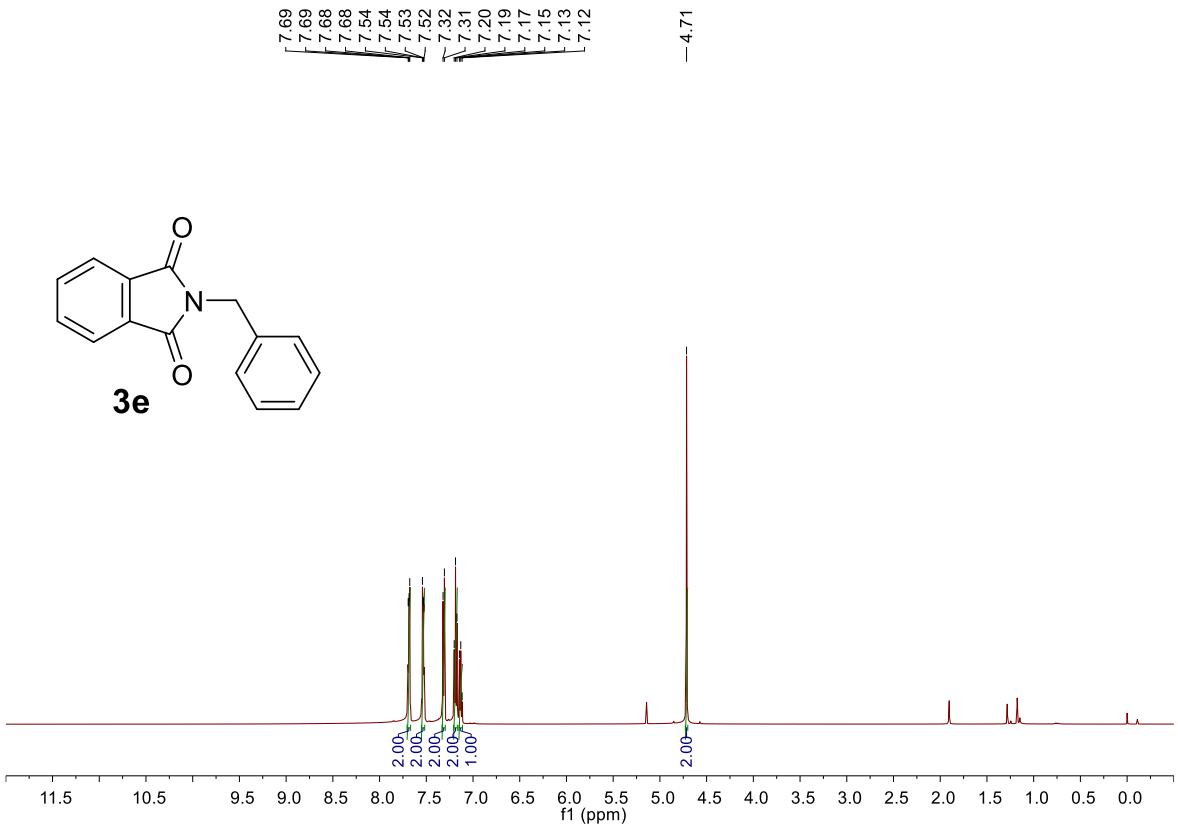
7.69
7.69
7.68
7.68
7.54
7.54
7.53
7.52
7.32
7.31
7.20
7.19
7.17
7.15
7.13
7.12
4.71
O
N
O
3e
2.00
2.00
2.00
2.00
1.00
2.00
11.5 10.5 9.5 9.0 8.5 8.0 7.5 7.0 6.5 6.0 5.5 5.0 4.5 4.0 3.5 3.0 2.5 2.0 1.5 1.0 0.5 0.0
f1 (ppm)

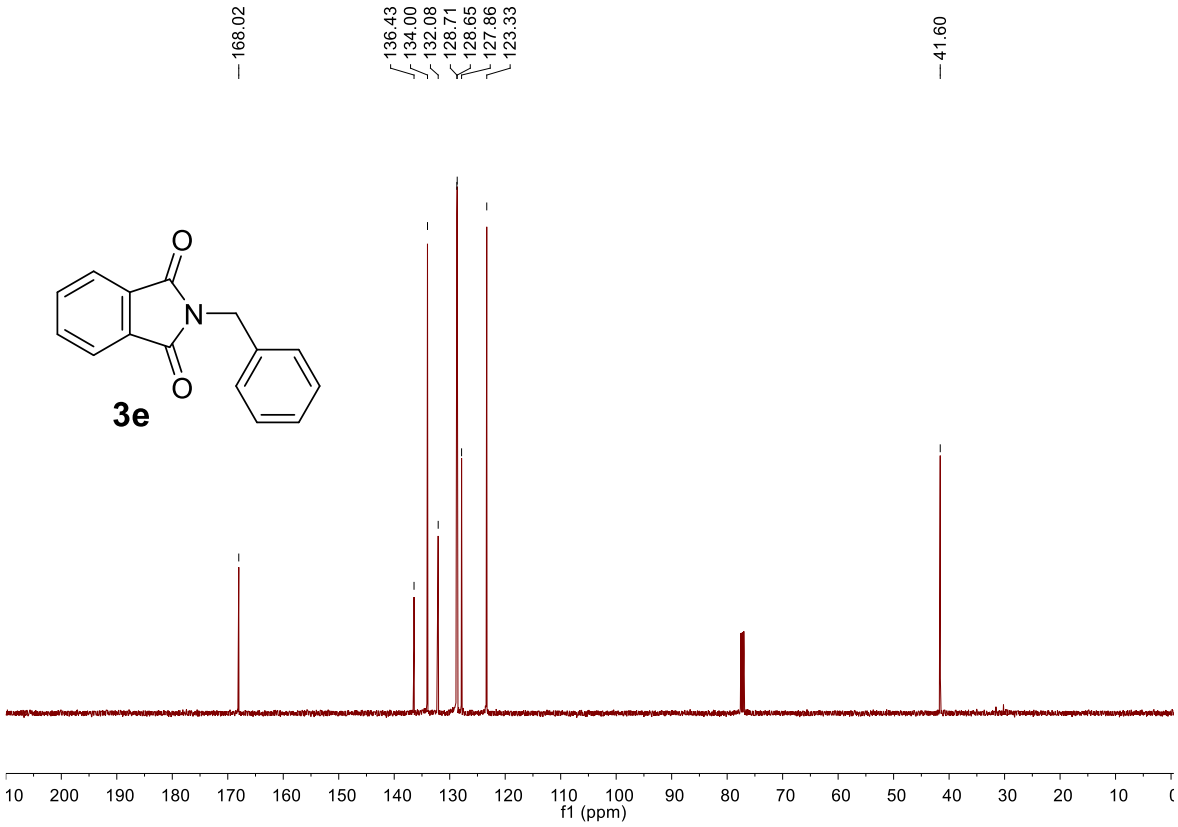
168.02
136.43
134.00
132.08
128.71
128.65
127.86
123.33
41.60
O
N
O
3e
10 200 190 180 170 160 150 140 130 120 110 100 90 80 70 60 50 40 30 20 10
f1 (ppm)

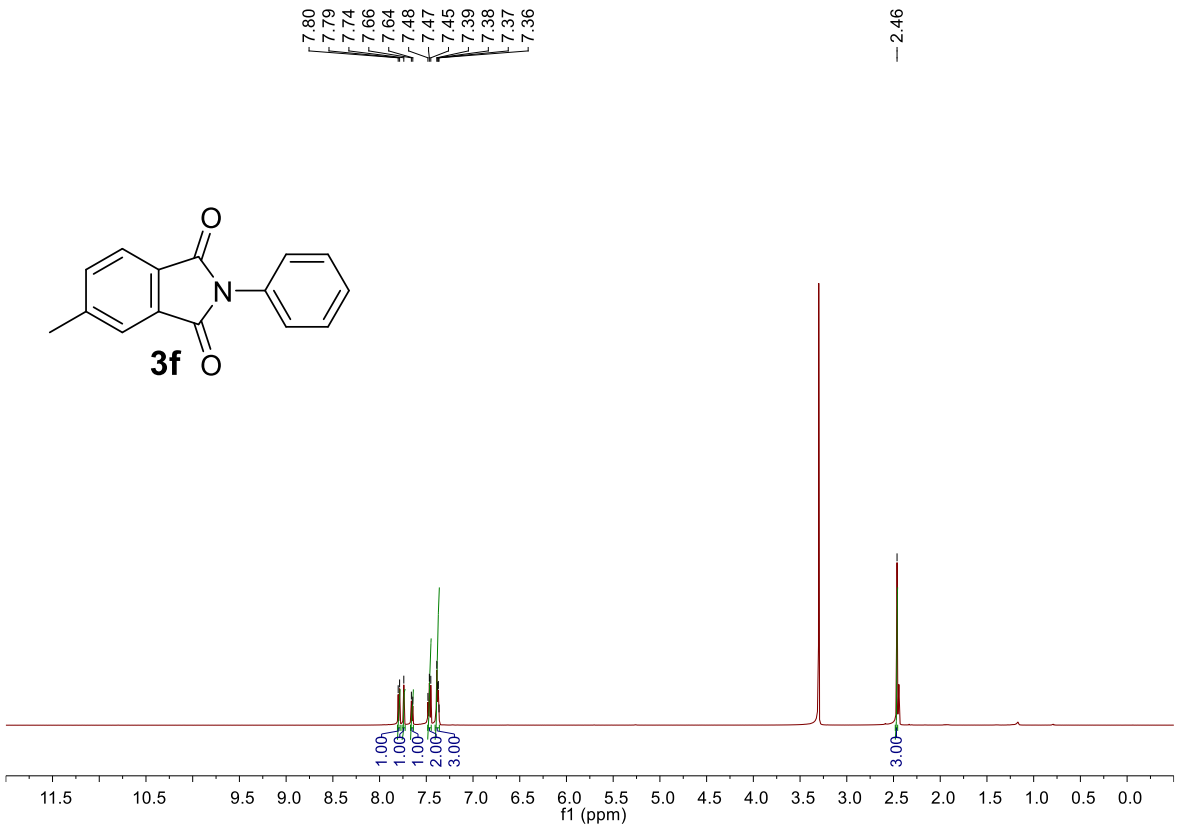
7.80
7.79
7.74
7.66
7.64
7.48
7.47
7.45
7.39
7.38
7.37
7.36
2.46
3f
1.00
1.00
1.00
2.00
3.00
3.00
11.5 10.5 9.5 9.0 8.5 8.0 7.5 7.0 6.5 6.0 5.5 5.0 4.5 4.0 3.5 3.0 2.5 2.0 1.5 1.0 0.5 0.0
f1 (ppm)

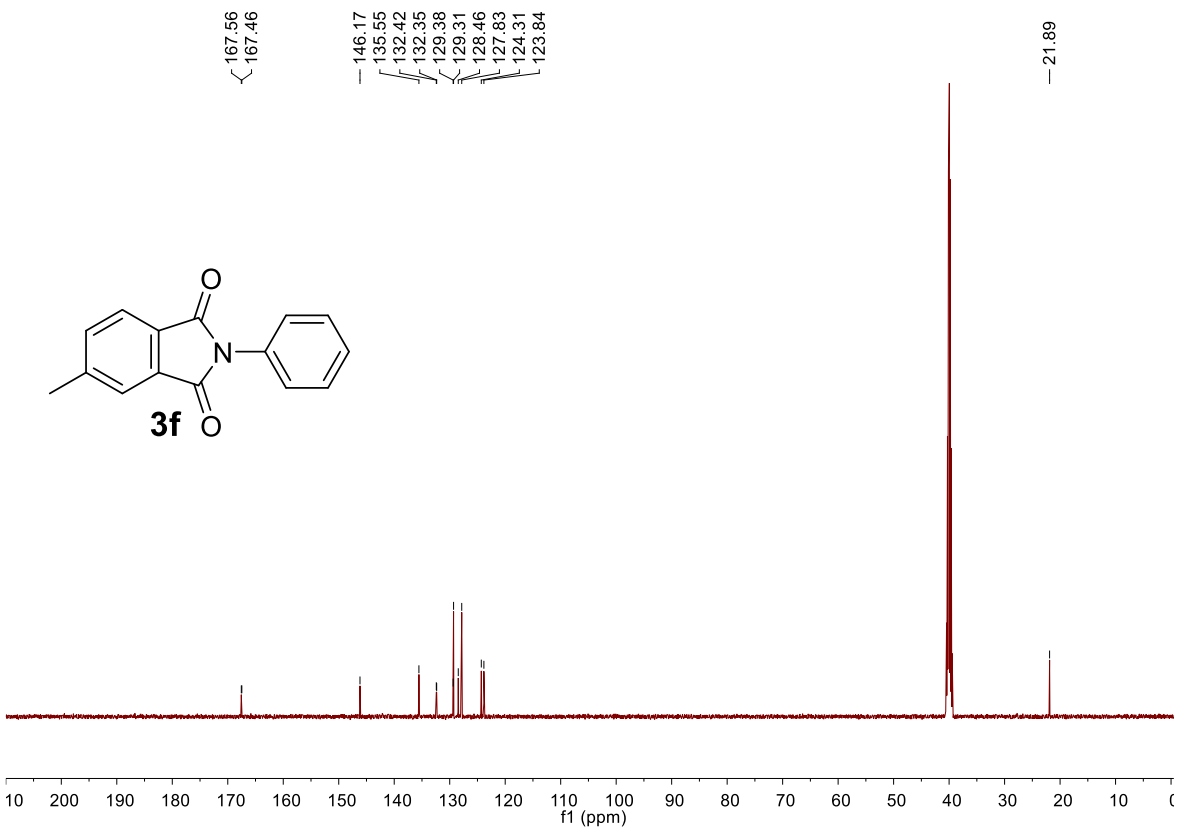
167.56
167.46
146.17
135.55
132.42
132.35
129.38
129.31
128.46
127.83
124.31
123.84
21.89
3f
10 200 190 180 170 160 150 140 130 120 110 100 90 80 70 60 50 40 30 20 10
f1 (ppm)

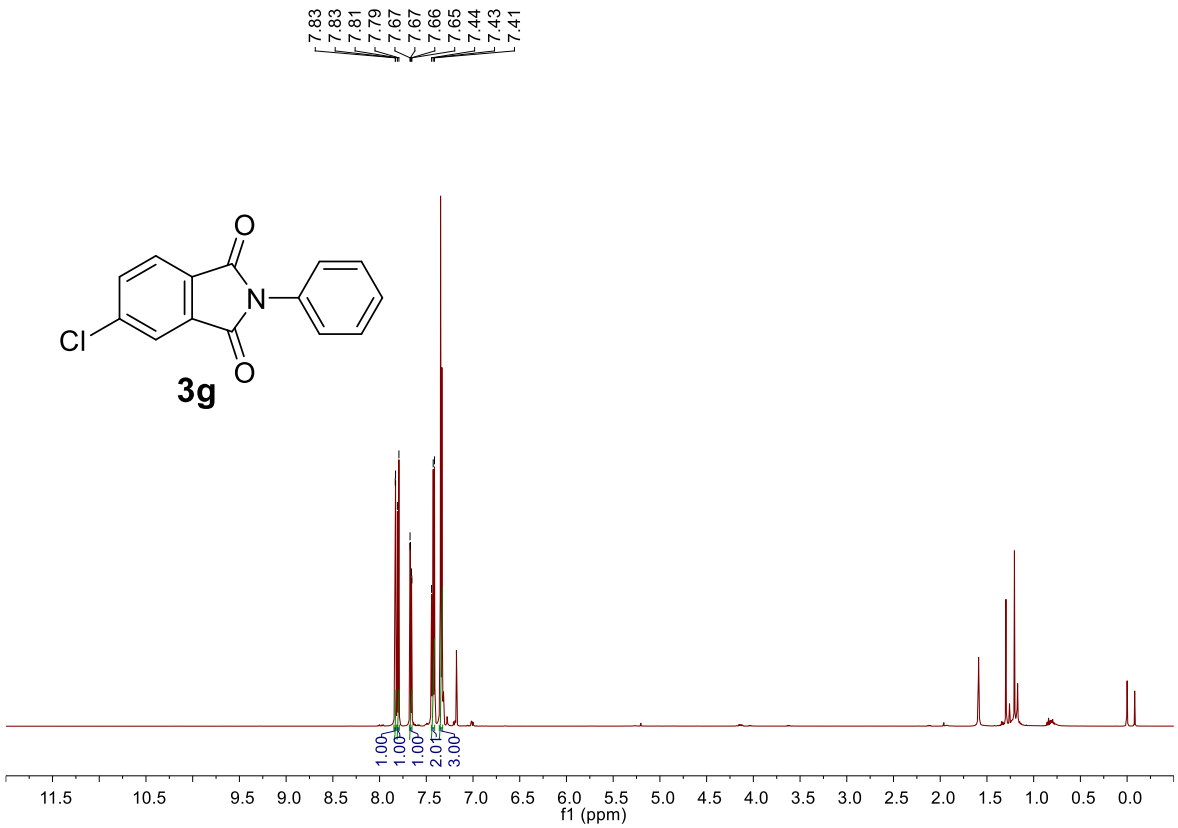
7.83
7.83
7.81
7.79
7.67
7.67
7.66
7.65
7.44
7.43
7.41
O
N
Cl
O
3g
1.00
1.00
1.00
2.01
3.00
11.5 10.5 9.5 9.0 8.5 8.0 7.5 7.0 6.5 6.0 5.5 5.0 4.5 4.0 3.5 3.0 2.5 2.0 1.5 1.0 0.5 0.0
f1 (ppm)

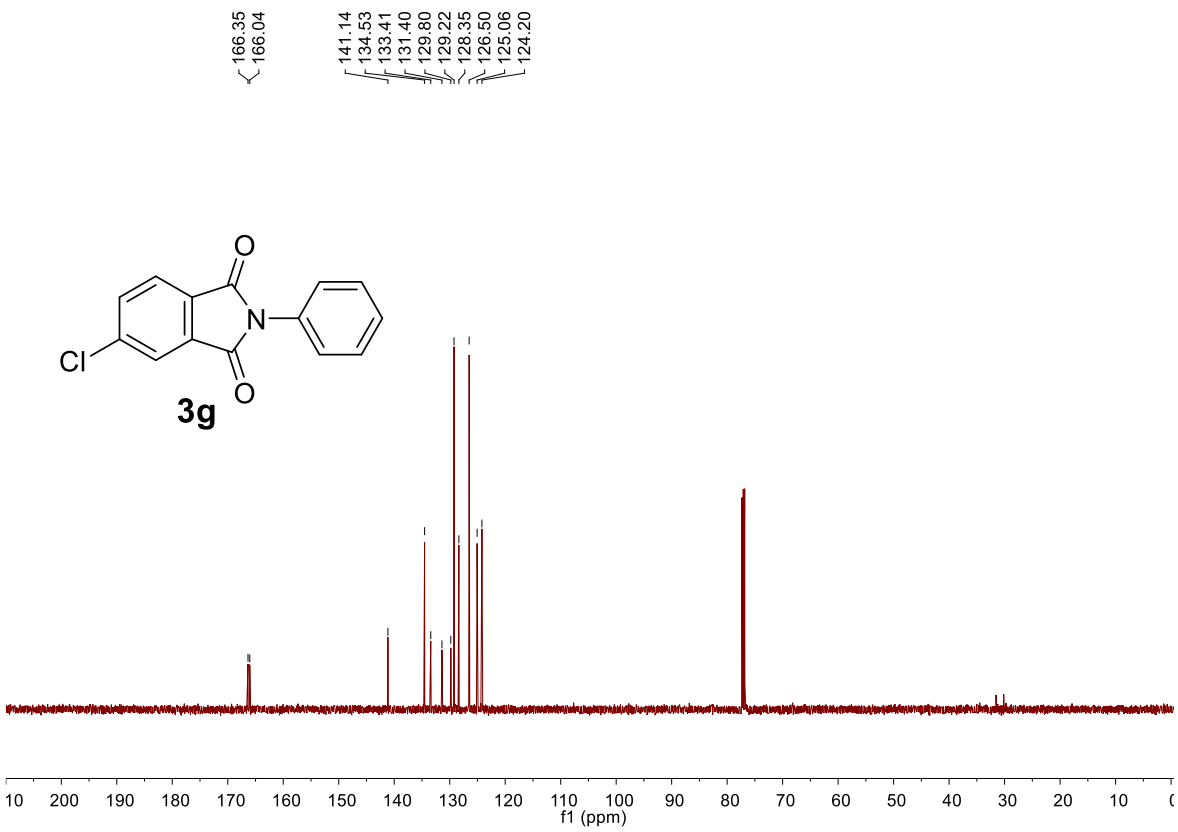
166.35
166.04
141.14
134.53
133.41
131.40
129.80
129.22
128.35
126.50
125.06
124.20
O
N
Cl
O
3g
10 200 190 180 170 160 150 140 130 120 110 100 90 80 70 60 50 40 30 20 10
f1 (ppm)

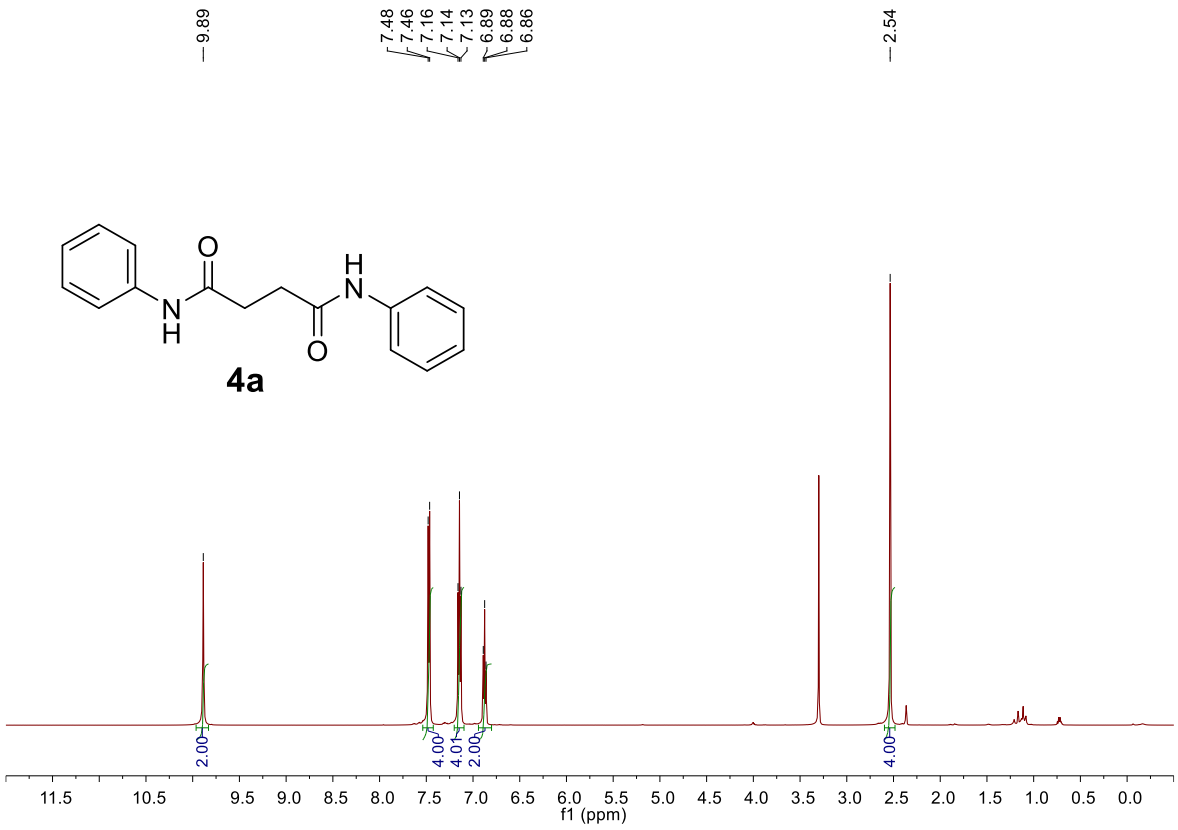
9.89
7.48
7.46
7.16
7.14
7.13
6.89
6.88
6.86
2.54
4a
2.00
4.00
4.01
2.00
4.00
11.5 10.5 9.5 9.0 8.5 8.0 7.5 7.0 6.5 6.0 5.5 5.0 4.5 4.0 3.5 3.0 2.5 2.0 1.5 1.0 0.5 0.0
f1 (ppm)

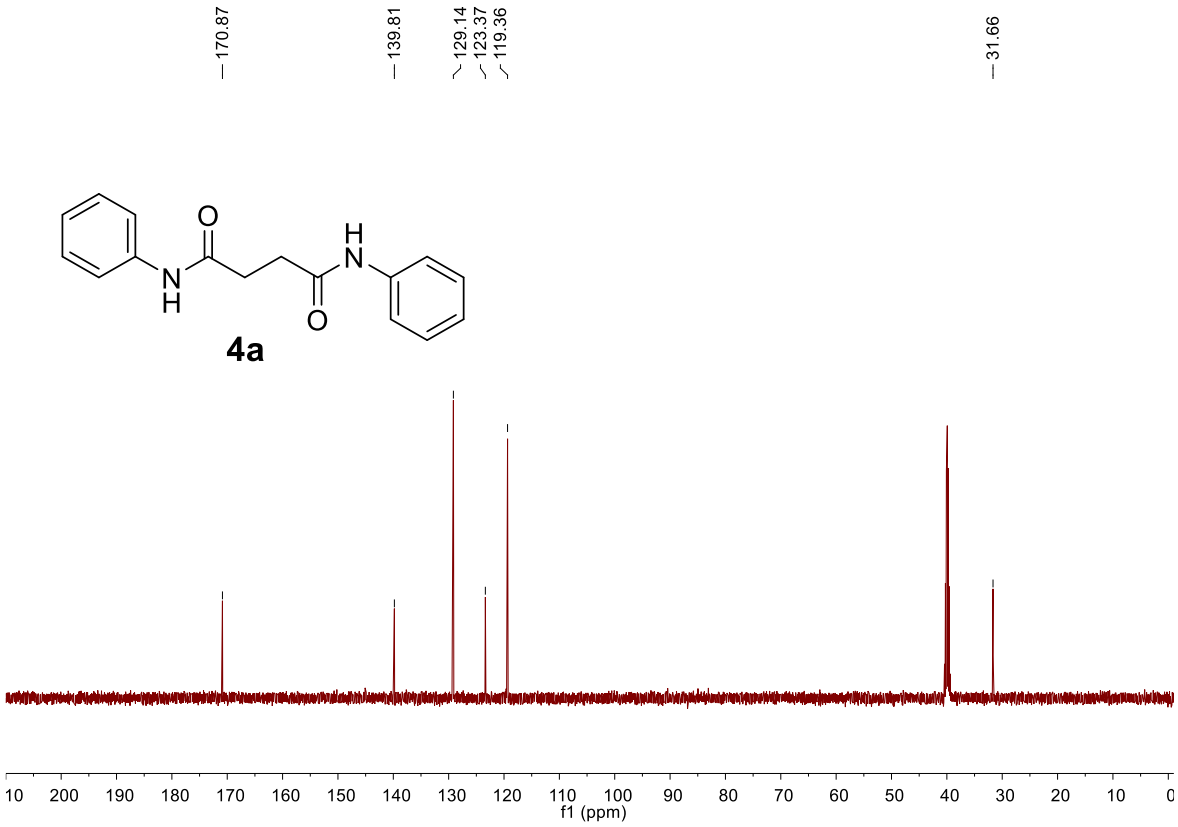
170.87
139.81
129.14
123.37
119.36
31.66
4a
10 200 190 180 170 160 150 140 130 120 110 100 90 80 70 60 50 40 30 20 10 0
f1 (ppm)

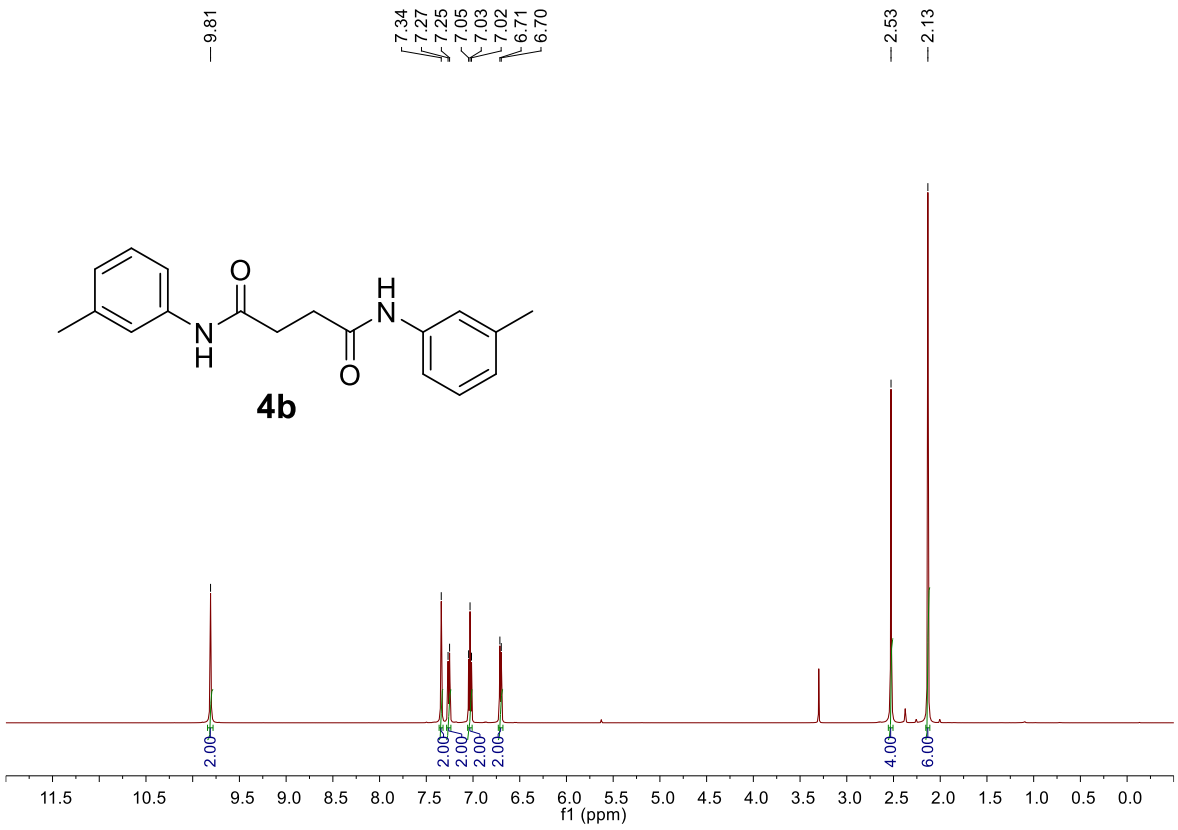
9.81
7.34
7.27
7.25
7.05
7.03
7.02
6.71
6.70
2.53
2.13
4b
2.00
2.00
2.00
2.00
2.00
4.00
6.00
11.5 10.5 9.5 9.0 8.5 8.0 7.5 7.0 6.5 6.0 5.5 5.0 4.5 4.0 3.5 3.0 2.5 2.0 1.5 1.0 0.5 0.0
f1 (ppm)

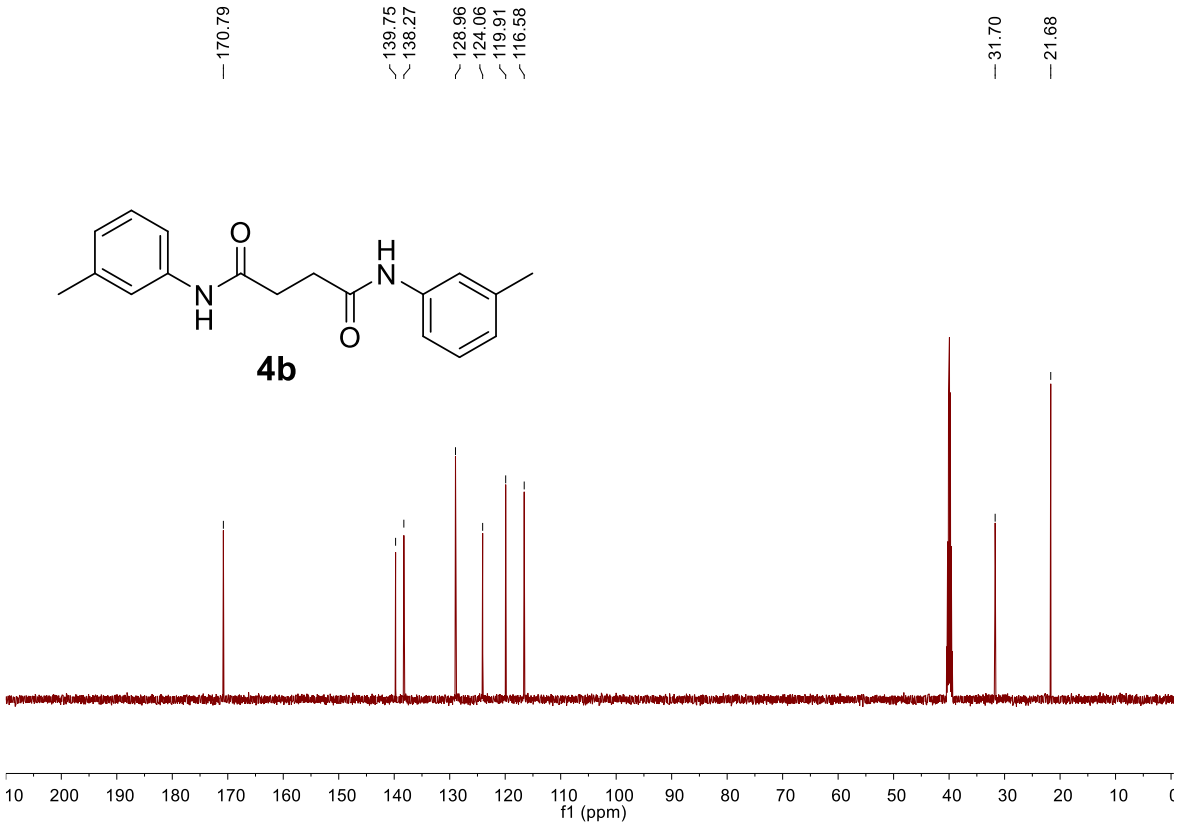
170.79
139.75
138.27
128.96
124.06
119.91
116.58
31.70
21.68
4b
10 200 190 180 170 160 150 140 130 120 110 100 90 80 70 60 50 40 30 20 10
f1 (ppm)

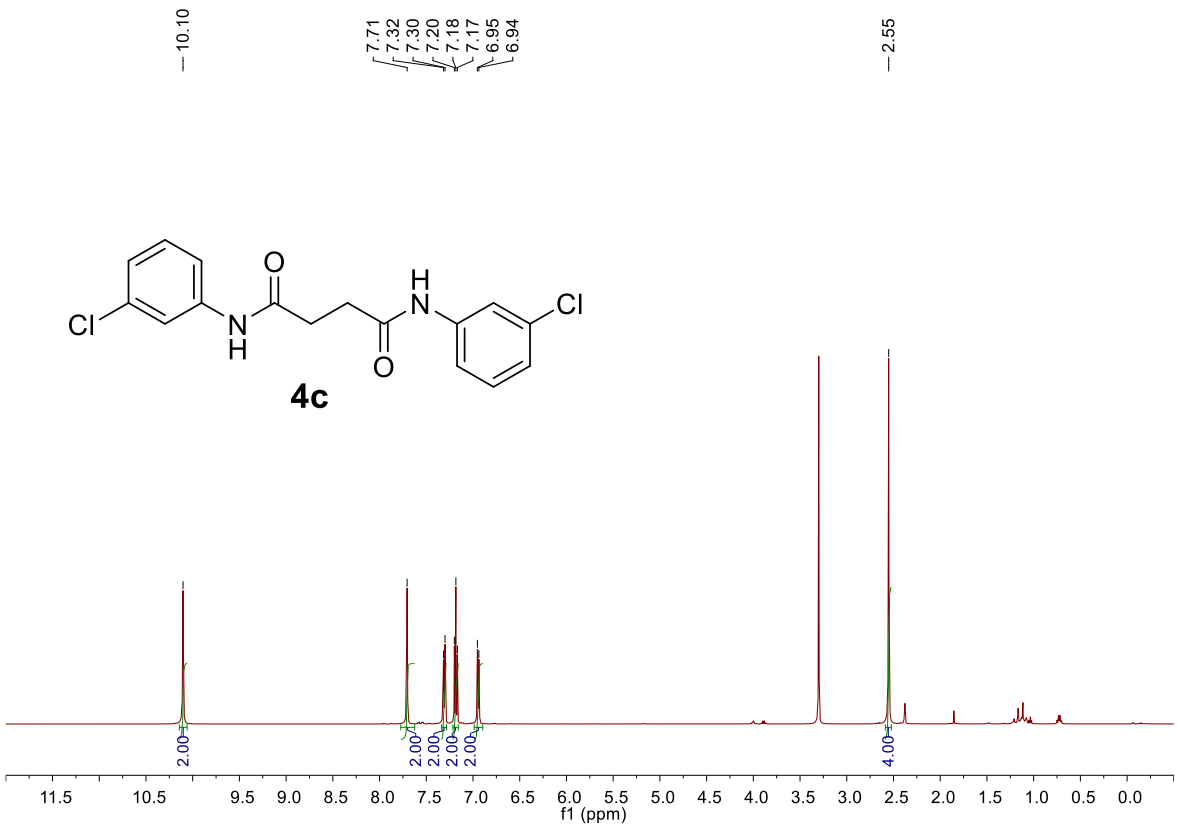
10.10
7.71
7.32
7.30
7.20
7.18
7.17
6.95
6.94
2.55
Cl
N
H
O
O
H
N
Cl
4c
2.00
2.00
2.00
2.00
2.00
4.00
11.5 10.5 9.5 9.0 8.5 8.0 7.5 7.0 6.5 6.0 5.5 5.0 4.5 4.0 3.5 3.0 2.5 2.0 1.5 1.0 0.5 0.0
f1 (ppm)

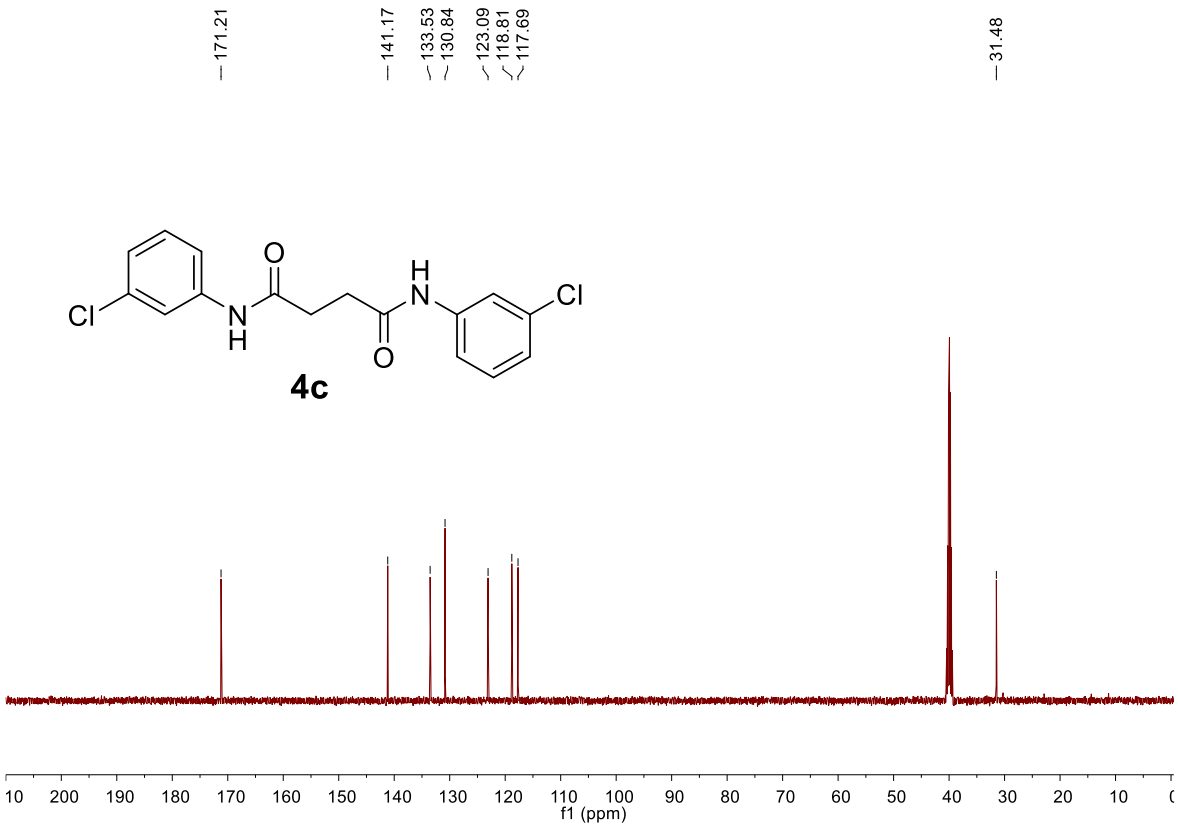
171.21
141.17
133.53
130.84
123.09
118.81
117.69
31.48
Cl
N
H
O
O
H
N
Cl
4c
200 190 180 170 160 150 140 130 120 110 100 90 80 70 60 50 40 30 20 10
f1 (ppm)

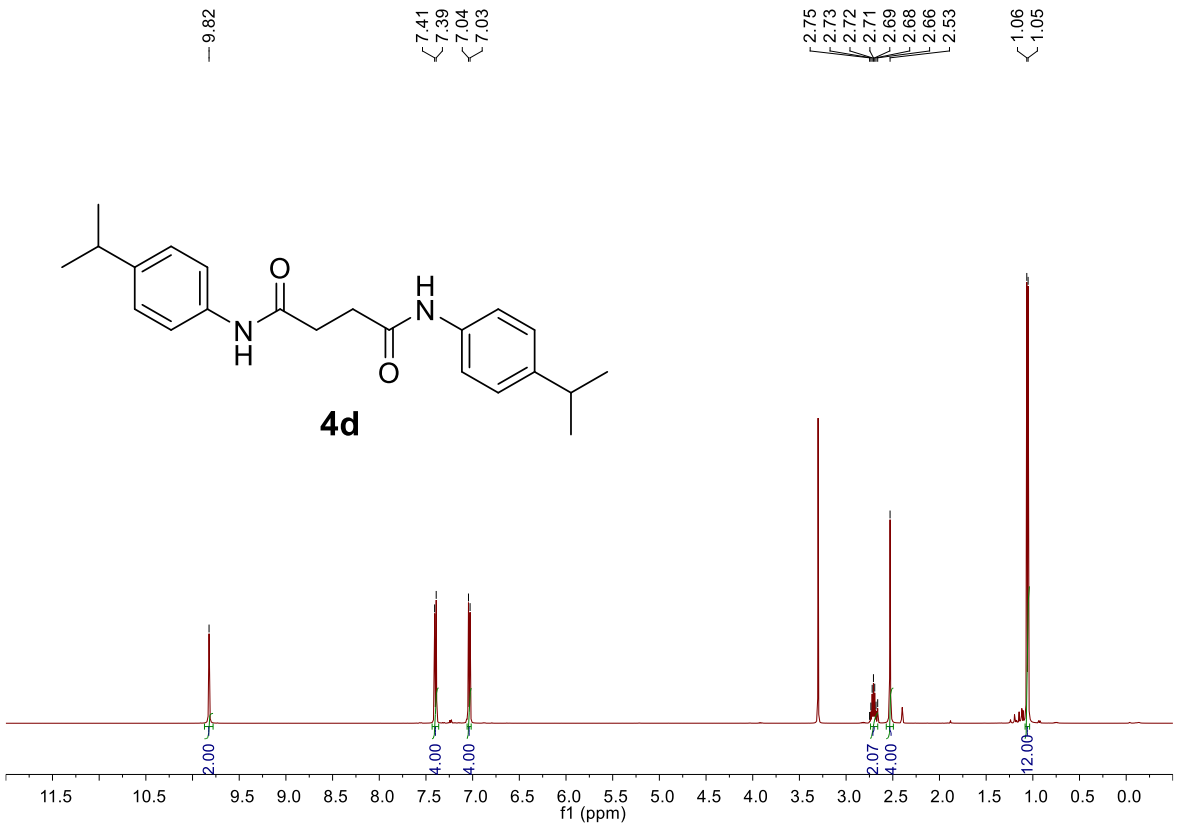
9.82
7.41
7.39
7.04
7.03
2.75
2.73
2.72
2.71
2.69
2.68
2.66
2.53
1.06
1.05
4d
2.00
4.00
4.00
2.07
4.00
12.00
f1 (ppm)

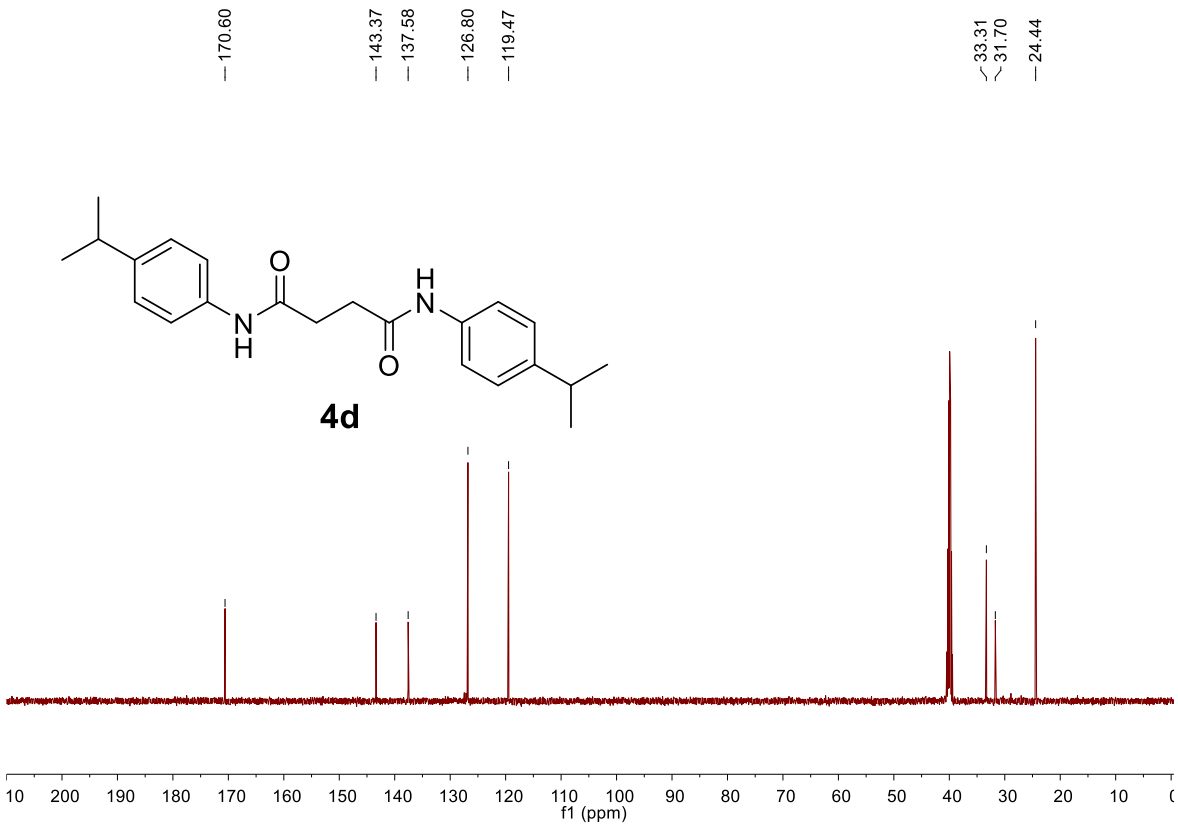
170.60
143.37
137.58
126.80
119.47
33.31
31.70
24.44
4d
f1 (ppm)

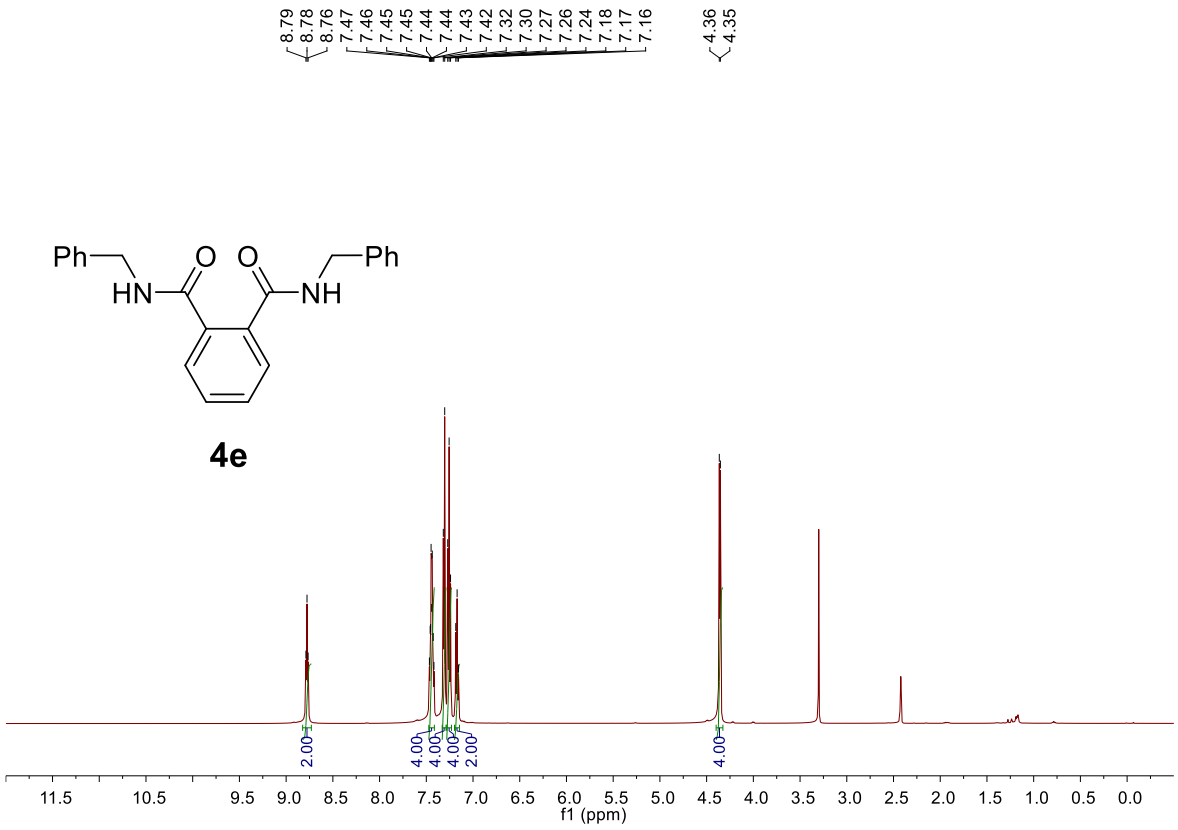
8.79
8.78
8.76
7.47
7.46
7.45
7.45
7.44
7.44
7.43
7.42
7.32
7.30
7.27
7.26
7.24
7.18
7.17
7.16
4.36
4.35
Ph
HN
O
O
NH
Ph
4e
2.00
4.00
4.00
4.00
2.00
4.00
11.5
10.5
9.5
9.0
8.5
8.0
7.5
7.0
6.5
6.0
5.5
5.0
4.5
4.0
3.5
3.0
2.5
2.0
1.5
1.0
0.5
0.0
f1 (ppm)

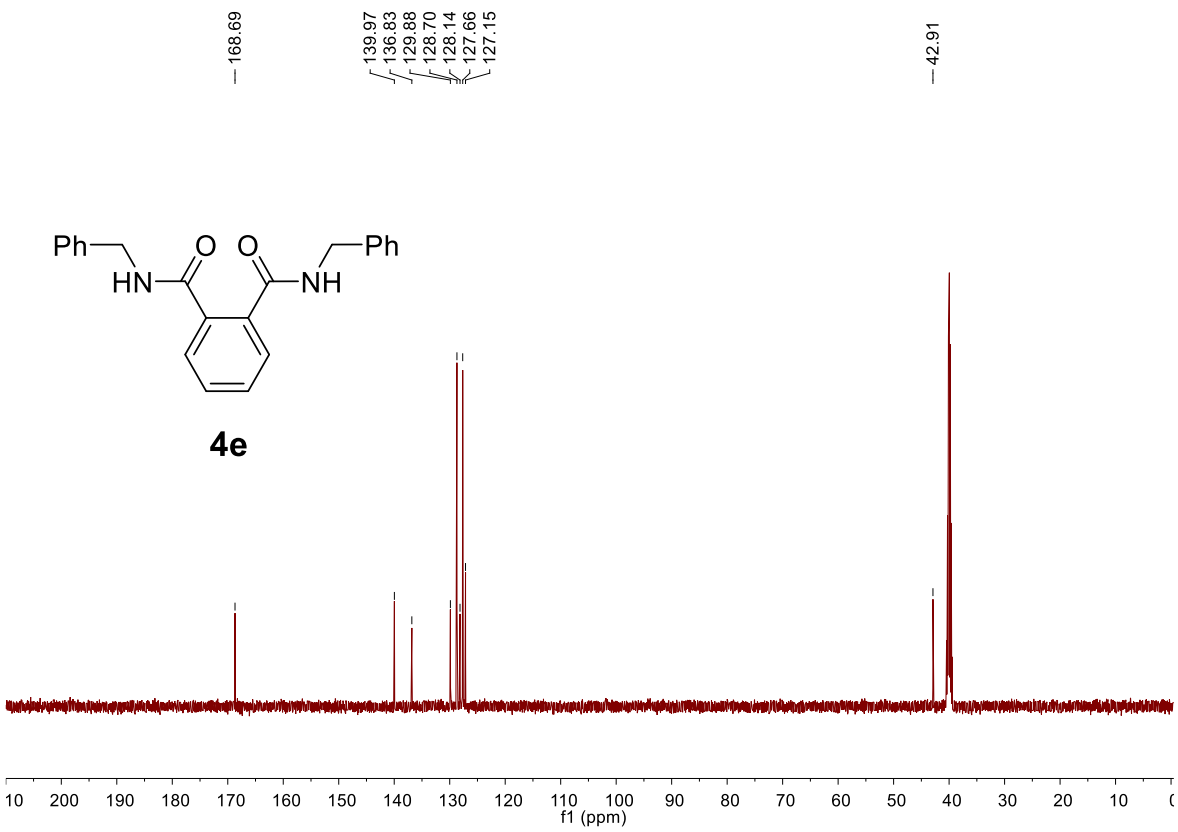
168.69
139.97
136.83
129.88
128.70
128.14
127.66
127.15
42.91
Ph
HN
O
O
NH
Ph
4e
200
190
180
170
160
150
140
130
120
110
100
90
80
70
60
50
40
30
20
10
f1 (ppm)

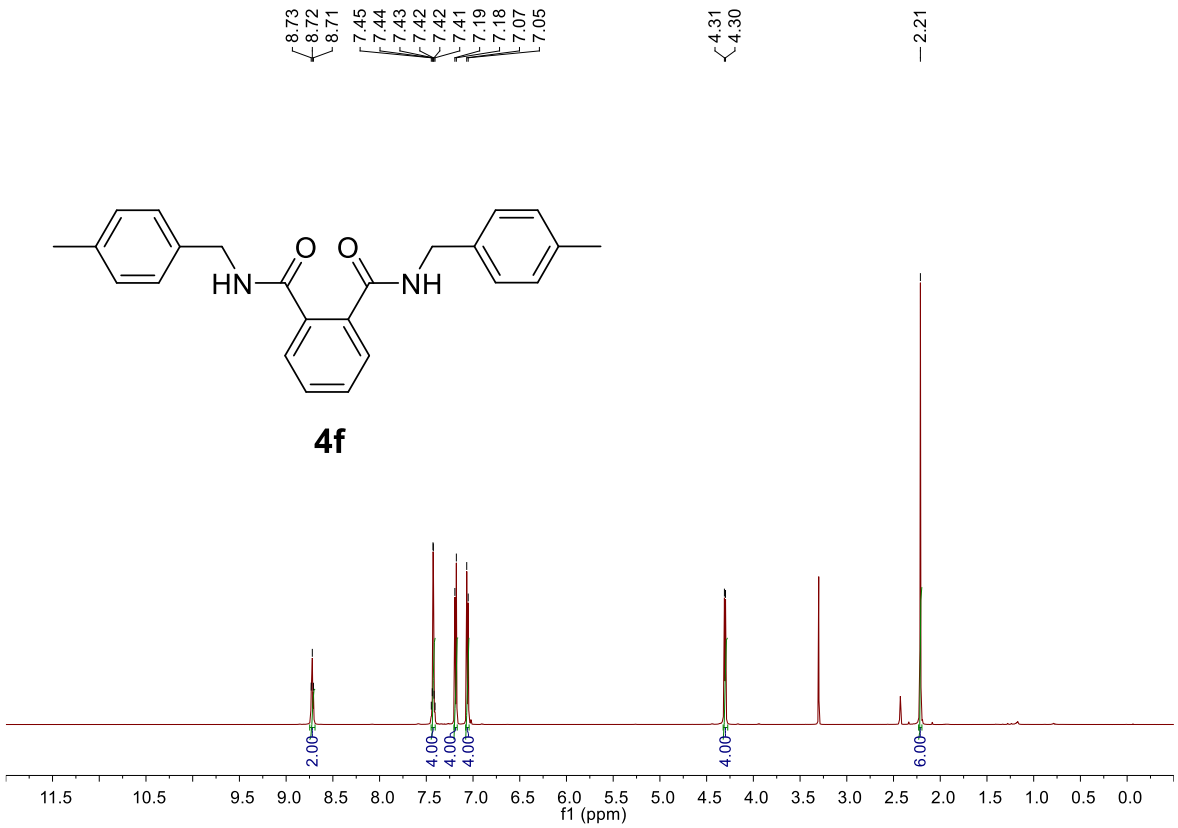
8.73
8.72
8.71
7.45
7.44
7.43
7.42
7.42
7.41
7.19
7.18
7.07
7.05
4.31
4.30
2.21
HN
O
O
NH
4f
2.00
4.00
4.00
4.00
4.00
6.00
11.5 10.5 9.5 9.0 8.5 8.0 7.5 7.0 6.5 6.0 5.5 5.0 4.5 4.0 3.5 3.0 2.5 2.0 1.5 1.0 0.5 0.0
f1 (ppm)

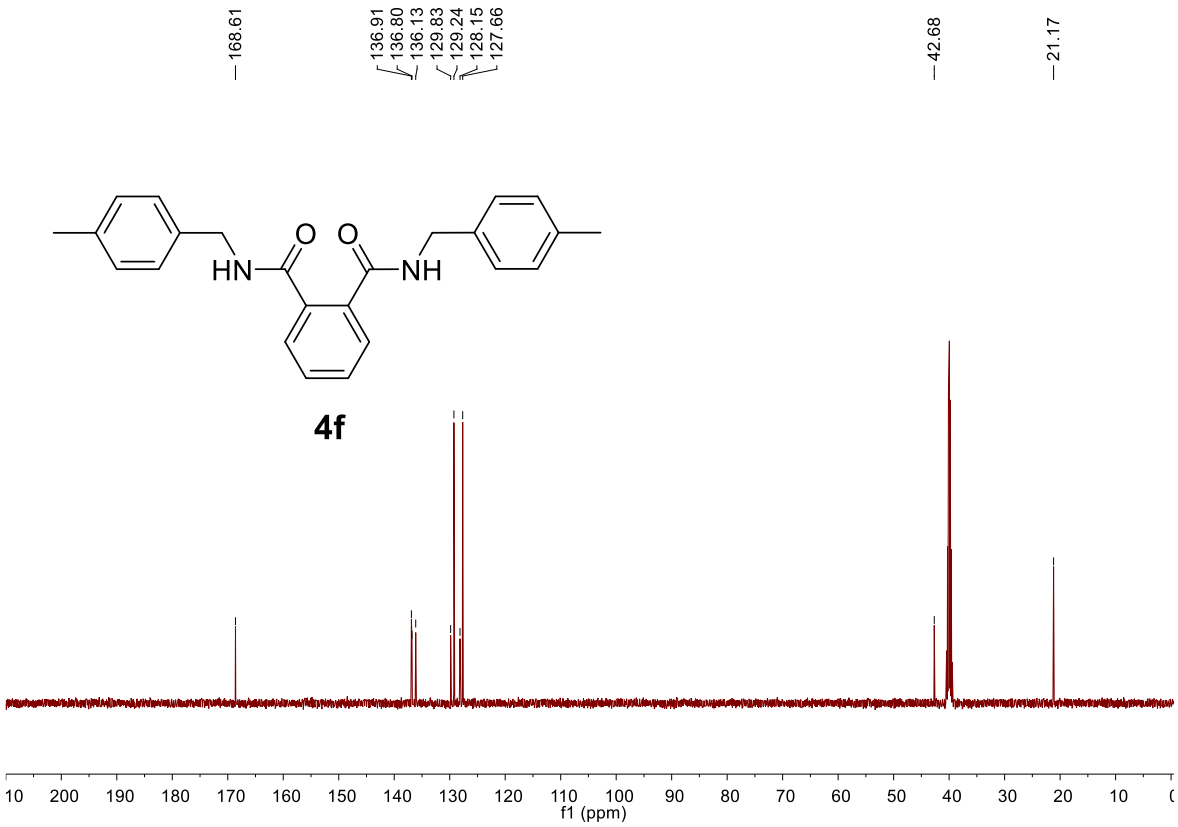
168.61
136.91
136.80
136.13
129.83
129.24
128.15
127.66
42.68
21.17
HN
O
O
NH
4f
10 200 190 180 170 160 150 140 130 120 110 100 90 80 70 60 50 40 30 20 10
f1 (ppm)

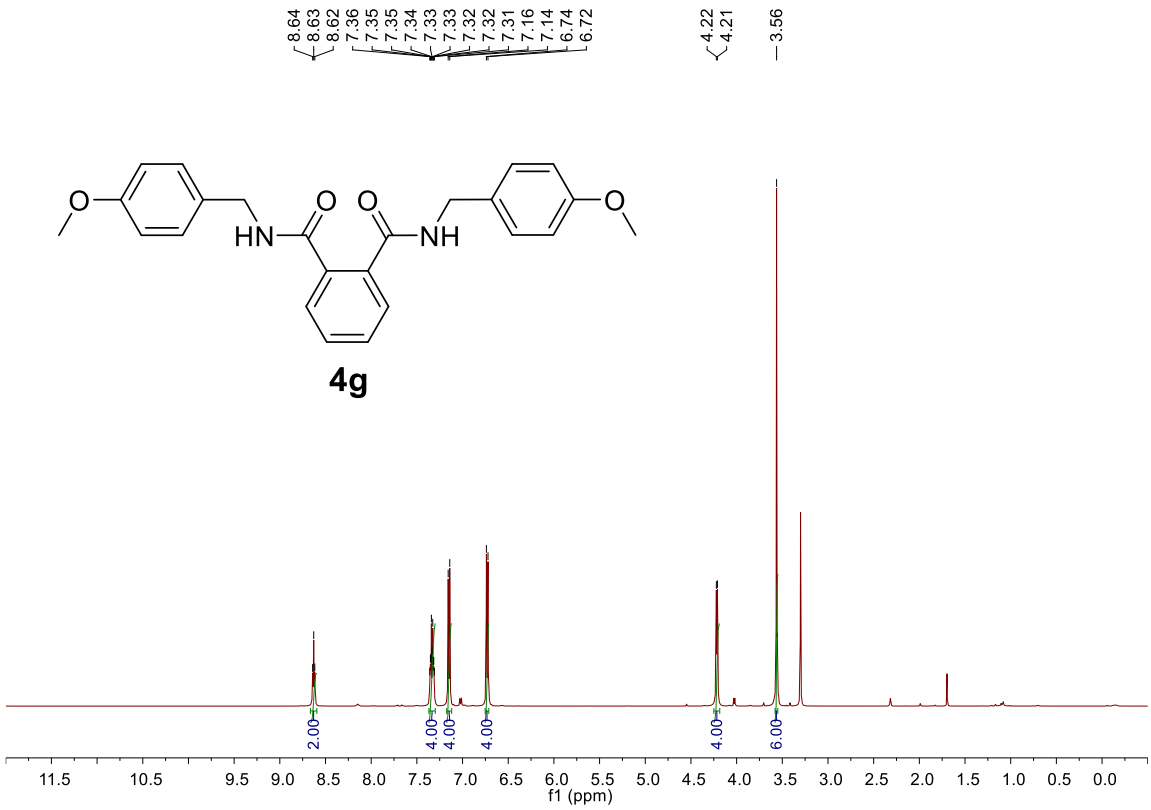
8.64
8.63
8.62
7.36
7.35
7.35
7.34
7.33
7.33
7.32
7.32
7.31
7.16
7.14
6.74
6.72
4.22
4.21
3.56
HN
NH
4g
2.00
4.00
4.00
4.00
4.00
6.00
f1 (ppm)

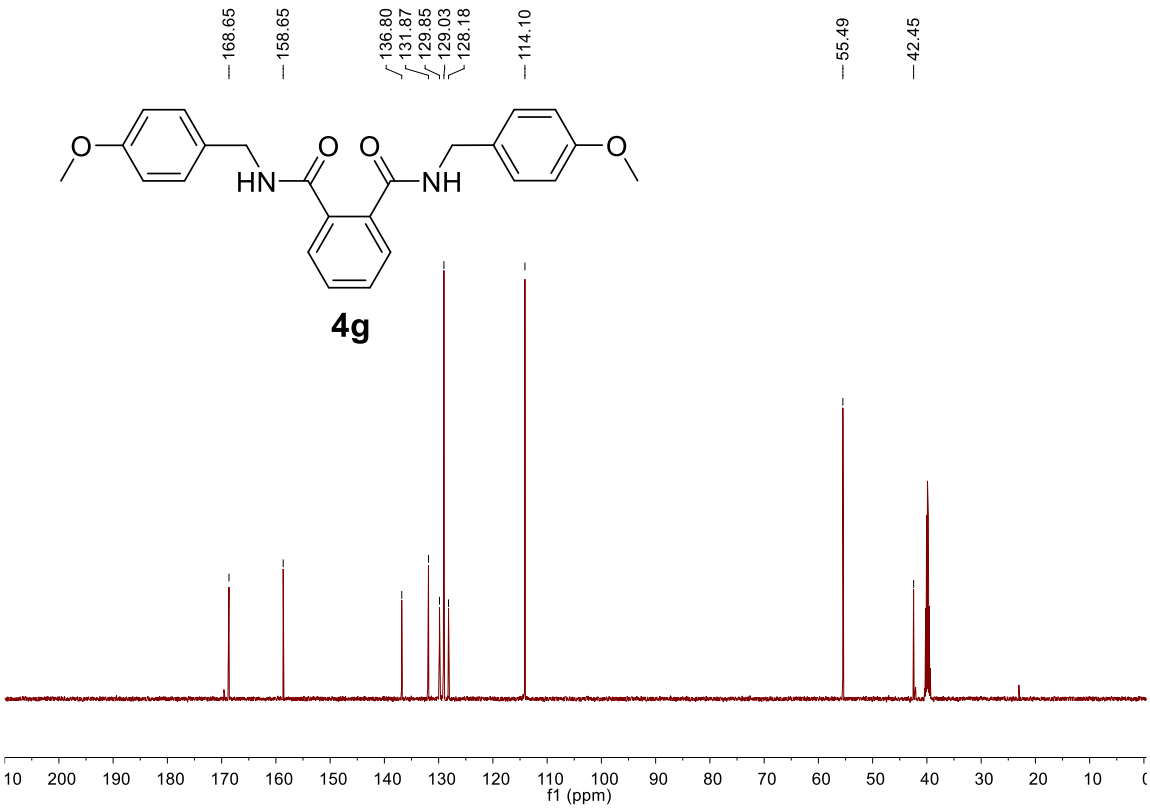
168.65
158.65
136.80
131.87
129.85
129.03
128.18
114.10
55.49
42.45
HN
NH
4g
f1 (ppm)

References

(S1) R. P. Bontchev, E. L. Venturini and M. Nyman, *Inorg. Chem.*, 2007, **46**, 4483–4491.

(S2) L. J. Bourhis, O. V. Dolomanov, R. J. Gildea, J. A. K. Howard and H. Puschmann, *Acta Crystallogr. Sect. A*, 2015, **71**, 59–75.

(S3) O. V. Dolomanov, L. J. Bourhis, R. J. Gildea, J. A. K. Howard and H. Puschmann, *J. Appl. Crystallogr.*, 2009, **42**, 339–341.

(S4) F. P. L. Lim, L. Y. Tan, E. R. T. Tiekinkb, A. V. Dolzhenko. *RSC Adv*. 2018, **8**, 22351−22360.

(S5) Ali, Md. A.; Moromi, S. K.; Touchy, A. S.; Shimizu, K. *ChemCatChem.* 2016, **8**, 891–894.

(S6) X. Wang, W. Xiong, Y. Huang, J. Zhu, Q. Hu, W. Wu, H. Jiang. *Org. Lett.* 2017, **19**, 5818−582.

(S7) R. Fu, Y. Yang, Y. Ma, F. Yang, J. Li, W. Chai, Q. Wang, R. Yuan. *Tetrahedron Lett.* 2015, **56**, 4527−4531.

(S8) R. Singudas, S. R. Adusumalli, P. N. Joshi, V. Rai. *Chem. Commun.* 2015, **51**, 473−476.